sustainability

MDPI

Article

Geoelectrical Characterization of Coastal Aquifers in Agbado-Ijaye, Lagos, Southwestern Nigeria; Implications for Groundwater Resources Sustainability

Kehinde D. Oyeyemi [1,*], Joyce Abuka-Joshua [1], Oluwatosin J. Rotimi [2], Bastien Dieppois [3], Modreck Gomo [4], Abayomi A. Olaojo [5], Philips O. Falae [6] and Mohamed Metwaly [7]

1 Applied Geophysics Programme, Department of Physics, Covenant University, Ota 112211, Nigeria
2 Department of Petroleum Engineering, Covenant University, Ota 112211, Nigeria
3 Center for Agroecology, Water and Resilience, Coventry University, Coventry CV1 2TU, UK
4 Faculty of Natural and Agricultural Sciences, Institute for Groundwater Studies, University of the Free State, Bloemfontein 9301, South Africa
5 Department of Earth Sciences, Ajayi Crowther University, Oke-Ebo 211271, Oyo, Nigeria
6 Department of Geology, Afe Babalola University, Ado-Ekiti 360101, Nigeria
7 Department of Archaeology, College of Tourism and Archaeology, King Saud University, Riyadh 11421, Saudi Arabia
* Correspondence: kehinde.oyeyemi@covenantuniversity.edu.ng

Abstract: Water is a natural resource; its availability depends on climatic and geological conditions, and it is invariably controlled by human activities. Agbado-Ijaye lies within a coastal area, where local communities have been facing incessant water shortages, especially during the dry season. This study investigated the groundwater-bearing geological unit(s) using hydrogeophysical techniques in the coastal environment. The electrical resistivity technique, involving vertical electrical sounding (VES) and two-dimensional (2D) electrical resistivity imaging via Wenner array electrode configuration, was used to characterize the geoelectric distribution. Twenty VES stations were investigated and current electrodes (AB/2 m) spacing expanded from 1–200 m; four 2D electrical resistivity imaging traverses having a length of 200 m each and interelectrode spacing of 10 m (level 1) to 60 m (level 6) was adopted. Four geoelectric units were delineated, namely: topsoil (15–251 Ωm), clayey (28–100 Ωm), clayey sand (125–190 Ωm) and sandy (205–876 Ωm) with thicknesses ranging from 0.7–1.3 m, 4.1–19.0 m, 2.6–15.6 m and undefined depth, respectively. The 2D imaging sections also detected similar geoelectric layers, corroborating the VES-derived sections. The inverted sections delineated two different aquifers: the shallower low-yield aquifer comprising sandy clay/clayey sand units with a maximum depth of about 5.5 m. This layer is adjudged to be the continental plain sand of the Benin Formation. The deeper high-yield aquifer with a maximum depth of 30.4 m is a beach sand unit that belongs to the Tertiary Alluvium of the Dahomey Basin. The study showed that hydrogeophysical investigation is vital in exploring, developing, and managing coastal groundwater resources.

Keywords: geoelectrical resistivity surveys; groundwater resources; coastal aquifer; Lagos; Nigeria

Citation: Oyeyemi, K.D.; Abuka-Joshua, J.; Rotimi, O.J.; Dieppois, B.; Gomo, M.; Olaojo, A.A.; Falae, P.O.; Metwaly, M. Geoelectrical Characterization of Coastal Aquifers in Agbado-Ijaye, Lagos, Southwestern Nigeria; Implications for Groundwater Resources Sustainability. *Sustainability* **2023**, *15*, 3538. https://doi.org/10.3390/su15043538

Academic Editor: Lucio Di Matteo

Received: 13 November 2022
Revised: 8 February 2023
Accepted: 9 February 2023
Published: 14 February 2023

1. Introduction

Groundwater is an important resource for many cities worldwide, and Lagos, Nigeria, is no exception. However, the city is facing several challenges in managing and sustainably utilizing its groundwater resources. The Lagos metropolis has significantly benefited from rapid industrialization from the early 90s, which has led to the geometrical progression of population growth [1]. The consequent increase in the demand for water resources due to uncontrollable urban migration has caused heavy reliance on groundwater resources for domestic and industrial uses because industrial effluents often severely pollute surface water. Overdrafting groundwater in the coastal area is responsible for seawater intruding into the aquifer system [2]. Lagos is a cosmopolitan city and rural-urban migration is

responsible for the population explosion, and Agbado-Ijaye is not left out of this social order. The economic activities (domestic and industrial) have led to the overextraction of groundwater. This has led to the lowering of the water table and a decline in groundwater quality due to pollution from saltwater intrusion and industrial effluents. Groundwater is an essential water source [3,4] and it is crucial to sustainable development by providing low-cost and high-quality water supplies. However, there is a lack of regulations to manage groundwater extraction and usage in Lagos state, Nigeria [5]. Additionally, there is a lack of enforcement of existing regulations prohibiting the contamination of the resource with industrial effluents [5,6]. Previous studies have shown that the long-term groundwater trends in Lagos have been declining [2,7,8] Water demand in Lagos has been reported to be approximately 724 million gallons per day, whereas 317 million gallons are being supplied, while the shortfall is 407 million gallons [2]. Then, over-reliance on groundwater as the possible alternative is accountable for the excessive withdrawal of this resource. About 20% of the world's freshwater supply is from groundwater, which constitutes about 0.61% of the entire world's water, including the oceans and permanent ice [9]. The role of groundwater and household water boreholes for domestic water provision in Lagos, Nigeria, and the entire Sub-Saharan Africa has been adjudged to be crucial to good sanitation, good health, and well-being [10,11]. They, therefore, advocated for good policies and regulations to ensure the sustenance of this natural resource. Groundwater sustainability has been defined as the development and use of groundwater resources so that they can be maintained for an indefinite period without causing unacceptable environmental, economic, or social consequences [12]. Therefore, the assessment, development and management of groundwater resources require adequate knowledge of subsurface aquifer systems. The aquifer's depth, geometry, petrophysical and hydraulic properties are crucial to groundwater yield and productivity. The electrical resistivity method for groundwater exploration has proven reliable in delineating such properties [13–17]. The technique has been successfully employed in delineating subsurface geological sequences, geological structures of interest, aquifer units, types and depth extent in almost all geological terrains [13–17].

Subsurface geoelectric sequences around the coastal environment using the electrical resistivity technique via vertical electrical sounding (VES) combined lithologic log [18]. The quality of the aquifer was established based on resistivity. One of the major problems encountered by the inhabitants of the coastal area is the nonavailability of fresh potable water [18]. The incursion of saline water into the aquifer contaminates the freshwater and renders it unfit for human consumption [18,19]. Integrated geoelectrical resistivity and geochemical techniques was employed to assess the risks of shallow aquifers to saltwater intrusion in the coastal belts of Lagos [19]. The groundwater quality in Matruh was examined using the physical property [20]. VES was instituted at 18 locations; this aided in delineating the geoelectric layer and establishing the fractured limestone sequence at depth. The approach used was adequate for demarcating geoelectric parameters and hydrogeological conditions. Electrical resistivity, induced polarization (IP), borehole logging and hydrochemical examination were employed in studying some coastal communities in Nigeria [2]. The depicted geoelectric layers were corroborated with the borehole logs and changes in the physicochemical properties around these communities were mapped out by the resistivity and IP contrast. The aquifer of a lateritic unit in Southwestern India was investigated using VES and chemical assessment of the water [21]. The aquifer within the porous soft lateritic unit has resistivity values less than 1400 Ωm and values $\leq$200 Ωm are tagged as groundwater-bearing zones [21]. The hydrochemical test suggests slightly acidic water originating from Ca-Mg-Cl and Na-Cl facies types [21]. The electrical resistivity technique is effective in groundwater–saltwater pollution studies within coastal environments due to its ability to differentiate between saline and freshwater based on its resistivity contrast [18–22].

The electrical resistivity data can delineate geological formations, such as aquifers, because of the contrasting electrical properties of the aquifer and that of the host rocks. Thus, resistivity surveys are often used to search for groundwater in porous media. Porous media are often related to sedimentary rocks such as clean sands and gravels, which have high porosity and make suitable aquifers. When saturated with freshwater, they can easily be differentiated from higher resistivity (poor aquifers), impermeable clays and marls [13–17]. As an essential tool in groundwater exploration, the surficial geophysical investigation is cost-effective in borehole construction by locating the target aquifer before drilling [23]. The intrusions of salt water into the coastal aquifer of the Lekki-Peninsula area of Lagos was delineated using the VES and borehole logs [24]. Twenty-five (25) VES data were used to map out freshwater aquifers in the Gbagada area of Lagos [25]. Geoelectrical resistivity and water level data from 30 hand-dug wells were used to monitor the rise in water levels and the impact on building structures and foundations [26]. The geoelectrical resistivity data were used to map out the groundwater level within the shallow aquifer in those areas.

Vertical electrical sounding (VES) data have been integrated with 2D electrical resistivity tomography to study groundwater exploration and contamination in sedimentary [14,17,19,24,27–30] and crystalline basement terrains within Southwestern Nigeria [31–35]. Within the Ota community in Southwestern Nigeria, resistivity soundings data were integrated with 2D ERT to reveal the geometry and characteristics of the sedimentary aquifer [27,28]. A time-lapse 2D ERT were conducted to observe the seasonal changes in groundwater quality and assessment around Olushosun dumpsite Lagos [29]. Also, VES and ERT were combined to assess the distribution of bitumen contaminants and their hazardous effects on groundwater around the Imakun-Omi community in the Eastern Dahomey basin of Southwestern Nigeria [30]. Within the crystalline basement terrain in Southwestern Nigeria, vertical electrical soundings were integrated with multiple-gradient array acquired 2D geoelectrical resistivity imaging to delineate the basement aquifer within Iberokodo, Abeokuta, Southwestern Nigeria [31]. The research revealed the nature and spatial variability of weathered and fractured zones within the subsurface. Vertical electrical soundings and 2D geoelectrical imaging were conducted for groundwater exploration within the complex basement terrain of the Basiri community, Ado-Ekiti, Southwestern Nigeria [32,33]. They delineated the saprolite, saprock and fresh basement in the area. The delineated weathered and fractured zones within the saprock are essential to groundwater accumulation. Integrated electrical resistivity imaging with the hydrochemical method were used to study the groundwater contamination around a dumpsite in Ibadan, Southwestern Nigeria [34]. Groundwater within the upper saprolite aquifers of the crystalline basement terrain is often poor in quality and prone to contamination [33,34]. To further understand the local flow and transport processes within crystalline basement aquifers, a hydrogeophysical research observatory site with four test wells was established in the University of Ibadan campus, Southwestern Nigeria [35]. Their preliminary studies have shown the conceptual model and hydraulic heterogeneities of the groundwater aquifer at the site [35]. VES with remote sensing and GIS techniques were integrated to map and assess the level of saltwater contamination in shallow aquifers around the Lagos lagoons [36,37]. Their studies showed that groundwater around the Lagos lagoons' upstream part is better for irrigation than the downstream. The scarcity, contaminations and overexploitation of groundwater, groundwater contaminations, declination of water level and other related challenges are being faced all over Lagos state, Nigeria. This study directly responds to the groundwater problems encountered by the inhabitants of the Agbado-Ijaye area of Lagos. To get around this problem, there is a need to decipher the geologic sections and establish the probable groundwater-bearing units. To date, there has been less documented or reported work on the groundwater potential of this community. This study aims to utilize the electrical resistivity method to assess, explore and delineate the aquifer systems within the study area.

2. Location and Geologic Setting

The study area lies within the residential area of the Agbado-Ijaye area of Lagos mainland. The area is between latitudes 06°40′32″–06°40′41″ N and longitudes 003°17′26″–003°17′42″ E (Figure 1), with an elevation between 61 and 64 m above sea level. The area is a gently sloping, low-lying terrain in the humid tropical region [29]. Southwestern Nigeria, where the study area is located, has two major climatic seasons: the dry season from November to March and the rainy (or wet) season between April and October, with a slight break in August [38]. Within coastal regions, such as Lagos, occasional rainfall within the dry season is often witnessed. On average, Agbado-Ijaye receives mean annual precipitation amounts greater than 2000 mm, serving as a significant source of groundwater recharge in the area [38].

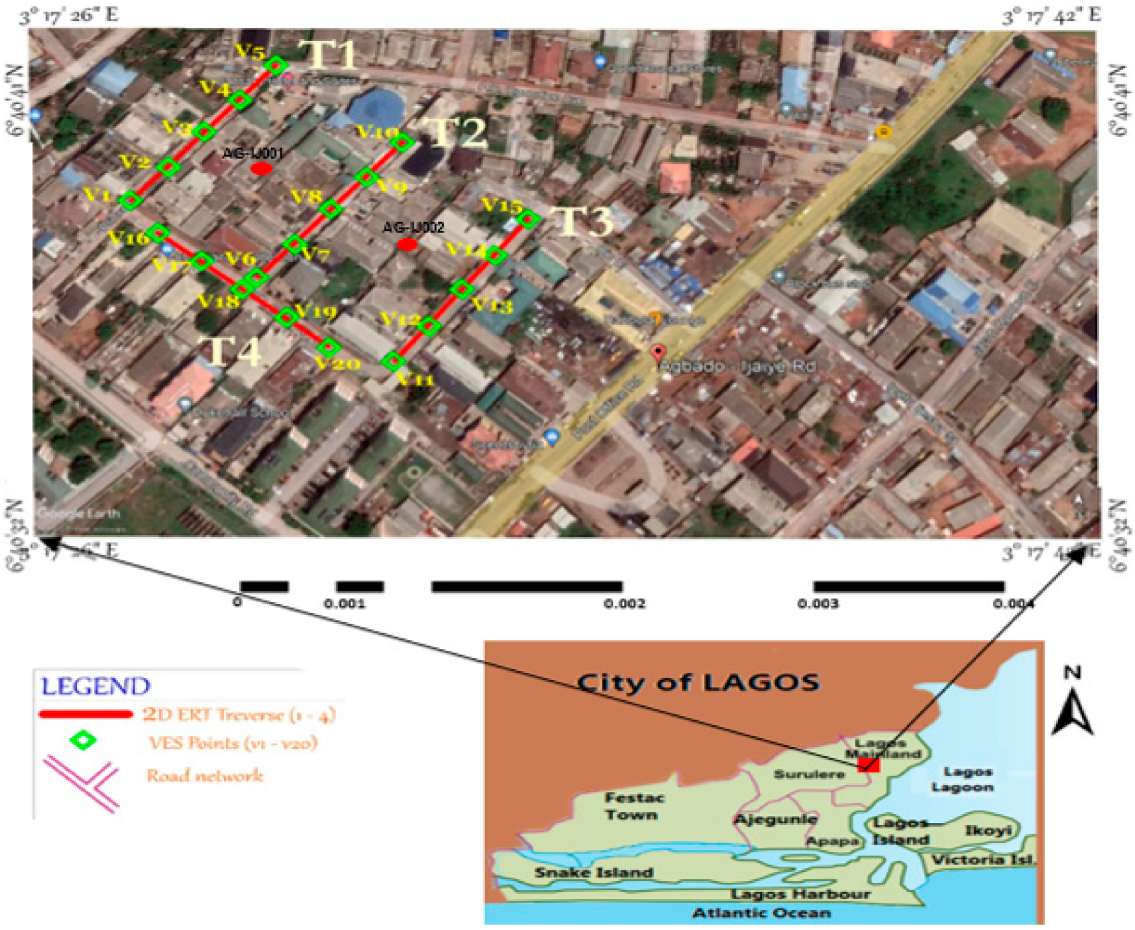

Figure 1. Location of the study area showing the VES points and 2D ERT profiles (T1–T4).

The cretaceous stratigraphy obtained from the outcrop and borehole records reveals that the subsurface in the study area (Figure 2) [39] is composed of the Abeokuta Group, subdivided into three formational units, namely Ise, Afowo and Araromi [40]. The Abeokuta Group is located directly above the base of the basement complex and Ewekoro, Akinbo, Oshosun, Ilaro, and Benin Formations overlie it. The Abeokuta Group consists mainly of poorly sorted ferrous grit, siltstone and mudstone with shale-clay layers [41–43]. The Akinbo Formation is the upper part of the shale overlaid by the Ewekoro limestone, which may be of the lowest Eocene period. The top of the formation is characterized by pure white, rough sand, and a little clay. The Akinbo Formation slowly moves into vast mud and is overlaid by the Oshosun Formation, typically Marine and Eocene. The Akinbo Formation is overlaid by the Oshosun Formation, which consists of the Eocene shale. The Ilaro Formation comprises a series of coarse sandy estuarine, deltaic, and continental beds.

The Ilaro Formation exhibits dramatic lateral shifts. Overlying the Ilaro Formation is the Benin Formation, primarily coastal plain sands and Tertiary alluvial deposits.

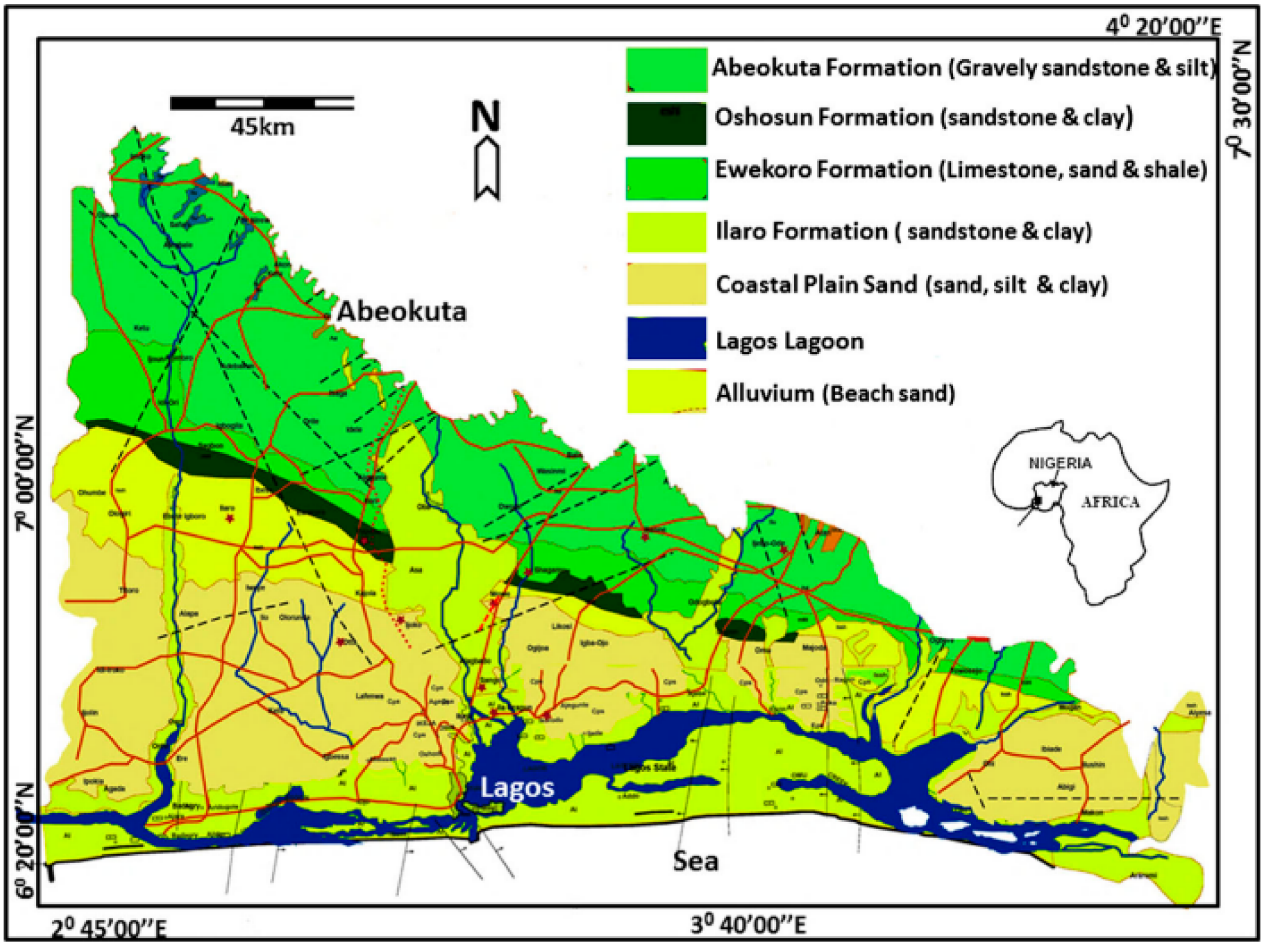

Figure 2. Geological map of the Nigerian part of the Dahomey Basin [39].

3. Materials and Methods

3.1. Data Acquisition and Field Procedures

A total of 20 vertical electrical soundings (VES) were acquired using an ABEM resistivity meter (SAS 4000) with a Schlumberger electrode configuration (Figure 3). The current electrode (AB/2 m) adopted for this investigation ranged from 1.0 to a maximum of 200 m. It was used due to the unavailability of space in the residential area. The spread was sufficient for the effective depth of investigation anticipated [44]. Precautions were taken to minimize electrode positioning errors as the surveys were conducted manually. A minimum stack of three and a maximum of six VES data was used for the VE-derived geoelectric section. In addition, we acquired four 200 m long 2D electrical resistivity tomography (ERT) traverses (T1–T4) with a Wenner array configuration and a minimum electrode spacing of 10 m (Figure 1). Several works have attested to the efficacy of the Wenner array to detect vertical distributions of subsurface resistivities, thereby being suitable for groundwater exploration in the sedimentary environment [45–49]. Level 1 involves interelectrode spacing of 10 m and the electrodes were moved collinearly by 10 m until the end of the traverse. At level 2, interelectrode spacing of 20 m was adopted and the movement was also 10 m. At levels 3, 4, 5 and 6, the interelectrode spacing of 30 m, 40 m, 50 m and 60 m were engaged, respectively, and the electrodes were moved by 10 m. Thus, the data were acquired up to a data level 6, with a maximum interelectrode spacing of 60 m on each profile. The length of each profile is 200 m, giving a total of 41 electrode positions

and 183 data points obtained for each traverse (T1–T4). The effective depth (Z_E) range, according to previous work [44], is approximately given as Equation (1):

$$Z_E = 0.190 \times \mathrm{AB} \quad (1)$$

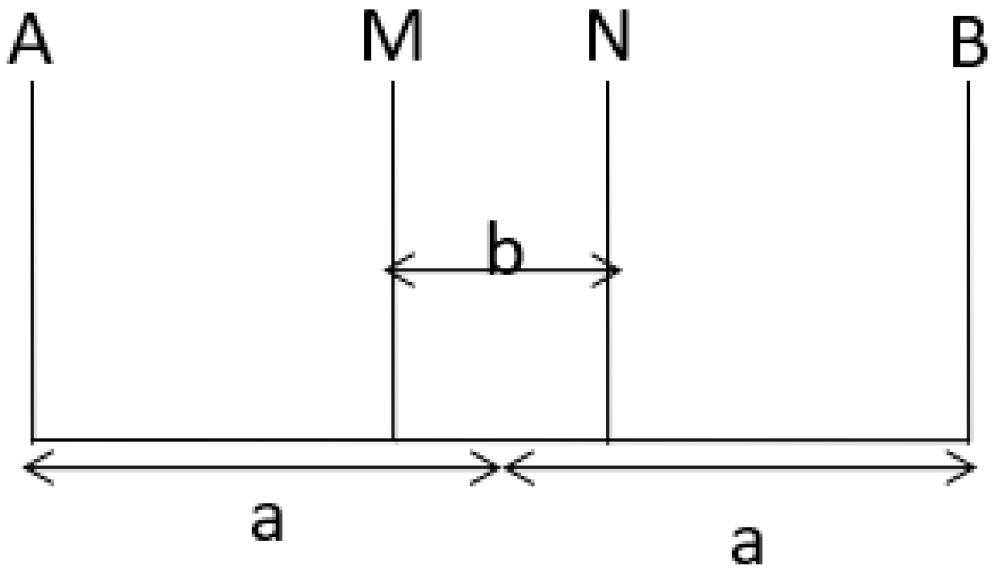

Figure 3. A Schlumberger array.

3.2. Data Processing and Inversion

The measured apparent resistivity data were processed manually by plotting the apparent resistivity values against the half-current electrode spacing (AB/2) or half the spread length, at each station on the bi-logarithmic graph (Figure 3). We employed a partial-curve-matching approach to obtain geoelectric parameters, such as several geoelectric layers and their respective resistivities and thicknesses, which were used as the initial models for the VES data. Subsequently, the resistivity data were iteratively processed and inverted using WinResist software. The iterative process attempted to improve the goodness of fit between the measured and computed data. The 2D ERT data were processed and inverted using the DIPRO software to produce the inversed resistivity model of the subsurface. The DIPRO inversion code uses a smoothness-constrained least-squares optimization technique to obtain the 2D distribution of the resistivity in the subsurface [50]. The algorithm subdivides the subsurface into several small rectangular blocks using a finite element model iteratively.

4. Results

4.1. Vertical Electrical Soundings

The representatives of inverse model resistivity curves obtained from the computer iteration of the resistivity soundings are presented in Figures 4 and 5. The geoelectric parameters for the VESs (T1-V1 to T1-V5) revealed three to four geoelectric layers, which vary from topsoil, clayey sand, clayey, and sandy horizons (Table 1). The corresponding geoelectric section constructed is presented in Figure 6. The first layer represents the topsoil with resistivity and thickness values that range between 88.2–251.4 Ωm and 0.8–1.2 m, respectively. From T1-V1 to T1-V3, the second identified layer denotes a clayey sand unit with resistivity and thickness values ranging between 132.2–176.4 Ωm and 2.6–15.6 m, respectively. While the second geoelectric layer in T1-V4 and T1-V5 is diagnostic of the clayey unit with resistivity and thickness values that range between 65.1–79.1 Ωm and 15.5–18.9 m, respectively.

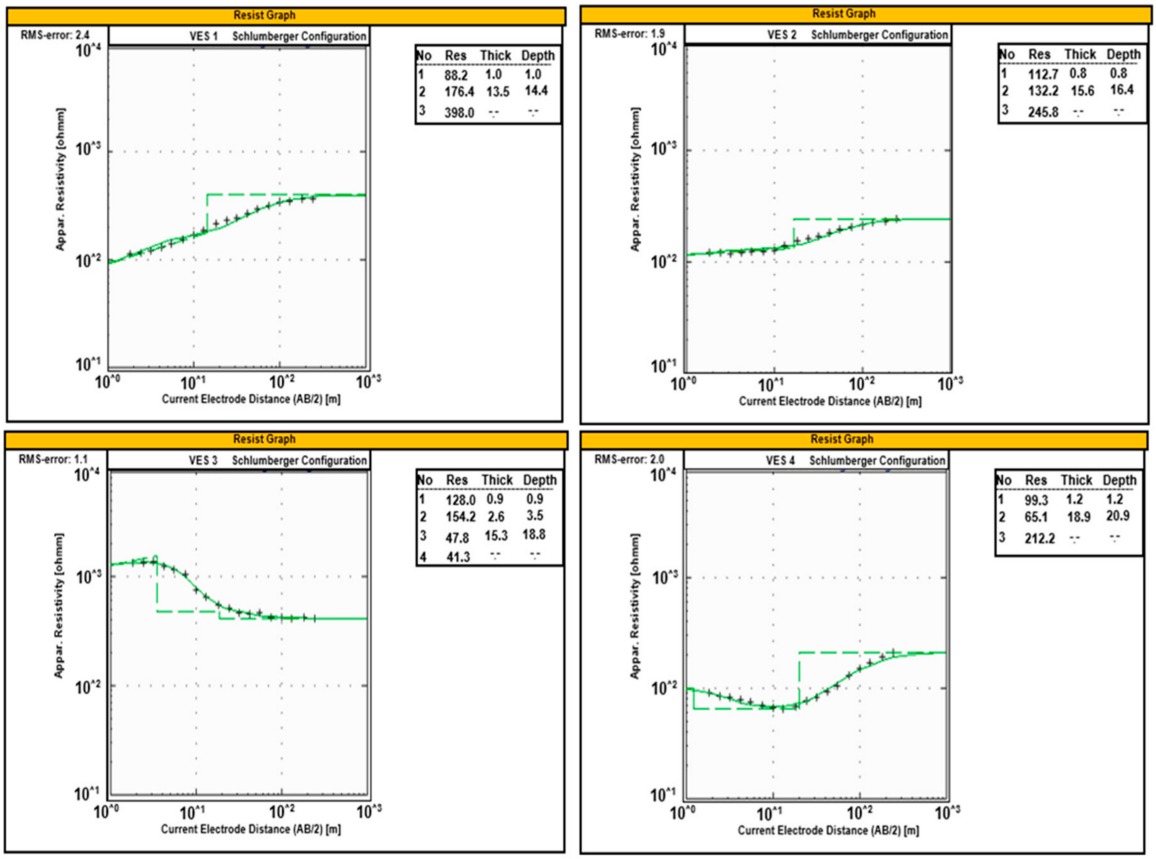

Figure 4. Representative vertical electrical sounding curves across traverse T1 (VESs 1–4). These soundings are conducted along the traverse line of the resistivity image Figure 9.

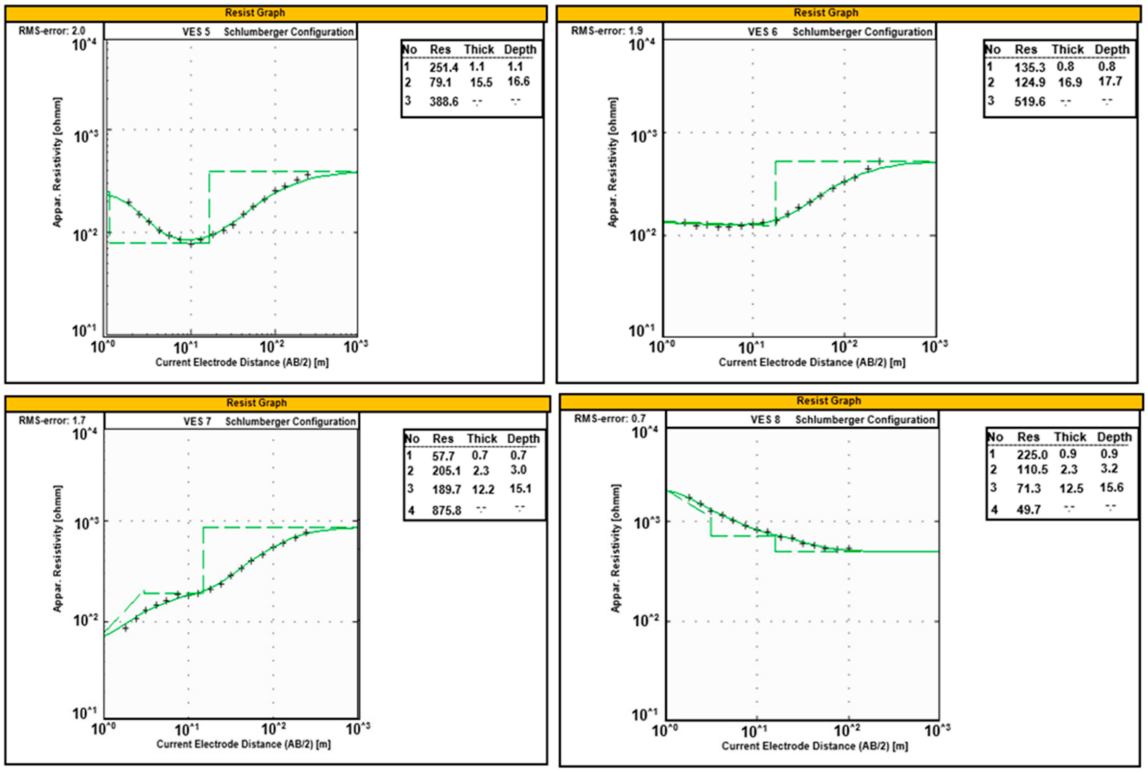

Figure 5. Representative vertical electrical sounding curves across traverse T2 (VESs 5–8). These soundings are conducted along the traverse line of the resistivity images Figures 9 and 10.

Table 1. Geoelectrical parameters of the vertical electrical sounding conducted along traverse T1.

Location	Elevation (m)	Layers	Resistivity (Ωm)	Thickness (m)	Depth (m)	Curve Type	Lithology
T1-V1	56 m	1 2 3	88.2 176.4 398.0	1.0 13.5 -	1.0 14.4 -	A	Topsoil Clayey Sand Sandy
T1-V2	58 m	1 2 3	112.7 132.2 245.8	0.8 15.6 -	0.8 16.4 -	A	Topsoil Clayey Sand Sandy
T1-V3	57 m	1 2 3 4	128.1 154.2 47.8 41.3	0.9 2.6 15.3 -	0.9 3.5 18.8 -	KQ	Topsoil Clayey Sand Clayey Clayey
T1-V4	56 m	1 2 3	99.3 65.1 212.2	1.2 18.9 -	1.2 20.1 -	H	Topsoil Clayey Sandy
T1-V5	57 m	1 2 3	251.4 79.1 388.6	1.1 15.5 -	1.1 16.6 -	H	Topsoil Clayey Sandy

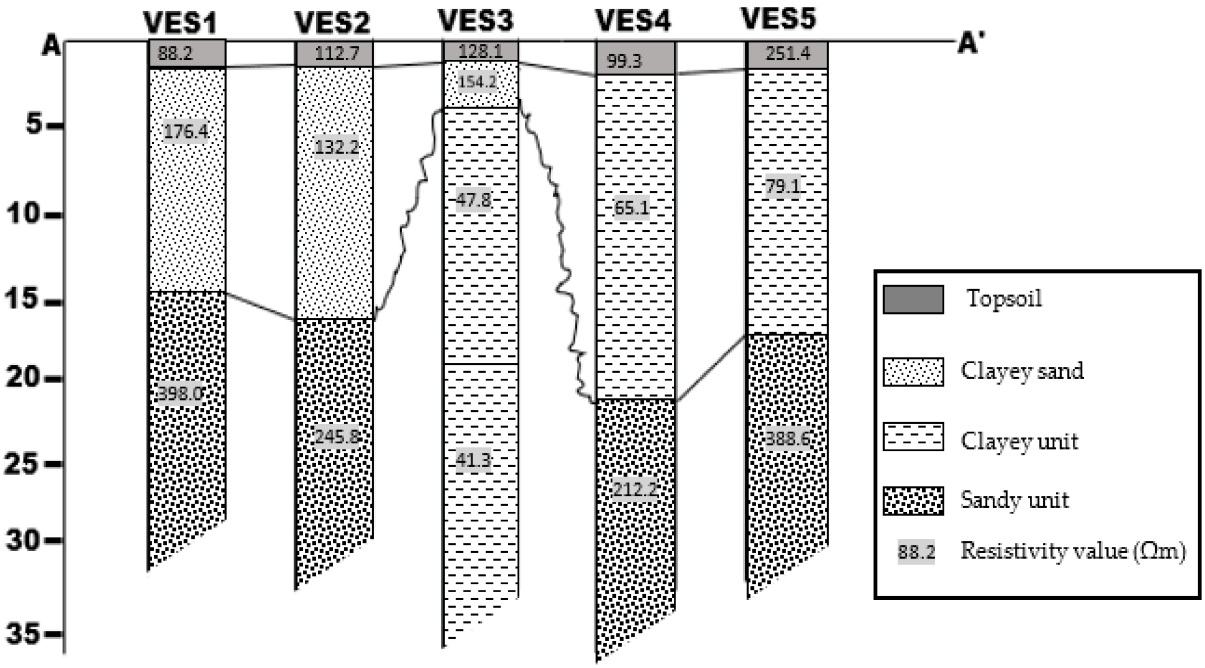

Figure 6. VES-derived geoelectric section from VESs (1–5) with resistivity values in Ohm-m.

Table 2 shows the geoelectric parameters and delineated layers for VESs (6–10) and the corresponding geoelectric section constructed is presented in Figure 7. The delineated geoelectric layers are about three to four, which vary from topsoil, clayey, clayey sand, and sandy horizons. The topsoil has resistivity and thickness values that vary between 57.7–225.0 Ωm and 0.7–0.9 m, respectively. The second layer across VES 6, VES 8 and VES 9 denote clayey to clayey sand units with resistivity values ranging from 70.2–124.9 Ωm and a layer thickness of 2.3–16.9 m. Also, the second identified layer in VES 7 indicates a sandy layer with resistivity and layer thickness values of 205.1 Ωm and 2.3 m, respectively. The second geoelectric layer beneath VES 10 depicts a clayey unit with resistivity and layer thickness values of 84.8 Ωm and 4.1 m, respectively. The third stratum in VES 6 is the sandy horizon with a resistivity value of 519.6 Ωm. Still, its layer thickness could not be determined because the current terminated on this horizon. Also, the third geoelectric layer beneath VESs 7 and 8 depicts clayey to clayey sand formations with resistivity and layer thickness values that range between 71.3–189.7 Ωm and 12.2–12.5 m, respectively.

Meanwhile, the third horizon identified in VES 9 and VES 10 is indicative of a clayey unit with resistivity and layer thickness values that range between 75.2–99.7 Ωm and 11.5–25.4 m, respectively. The last identified layer in VES 7, VES 9 and VES 10 is interpreted to be a sandy horizon with resistivity values ranging from 307.7–875.8 Ωm. However, the delineated last layer in VES 8 is interpreted to be the clayey unit with a resistivity value of 49.7 Ωm.

Table 2. Geoelectrical parameters of the vertical electrical sounding conducted along traverse T2.

Location	Elevation (m)	Layers	Resistivity (Ωm)	Thickness (m)	Depth (m)	Curve Type	Lithology
T2-V6	56 m	1	135.3	0.8	0.8	H	Topsoil
		2	124.9	16.9	17.7		Clayey Sand
		3	519.6	-	-		Sandy
T2-V7	58 m	1	57.7	0.7	0.7	KH	Topsoil
		2	205.1	2.3	3.0		Sandy
		3	189.7	12.2	15.1		Clayey Sand
		4	875.8	-	-		Compacted Sand
T2-V8	57 m	1	225.0	0.9	0.9	Q	Topsoil
		2	110.5	2.3	3.2		Clayey Sand
		3	71.3	12.5	15.6		Clayey
		4	49.7	-	-		Clayey
T2-V9	58 m	1	202.6	0.9	0.9	HA	Topsoil
		2	70.2	4.0	4.9		Clayey
		3	75.2	11.5	16.4		Clayey
		4	431.0	-	-		Sandy
T2-V10	56 m	1	79.9	0.9	0.9	A	Topsoil
		2	84.8	4.1	5.0		Clayey
		3	99.7	25.4	30.4		Clayey
		4	307.7	-	-		Sandy

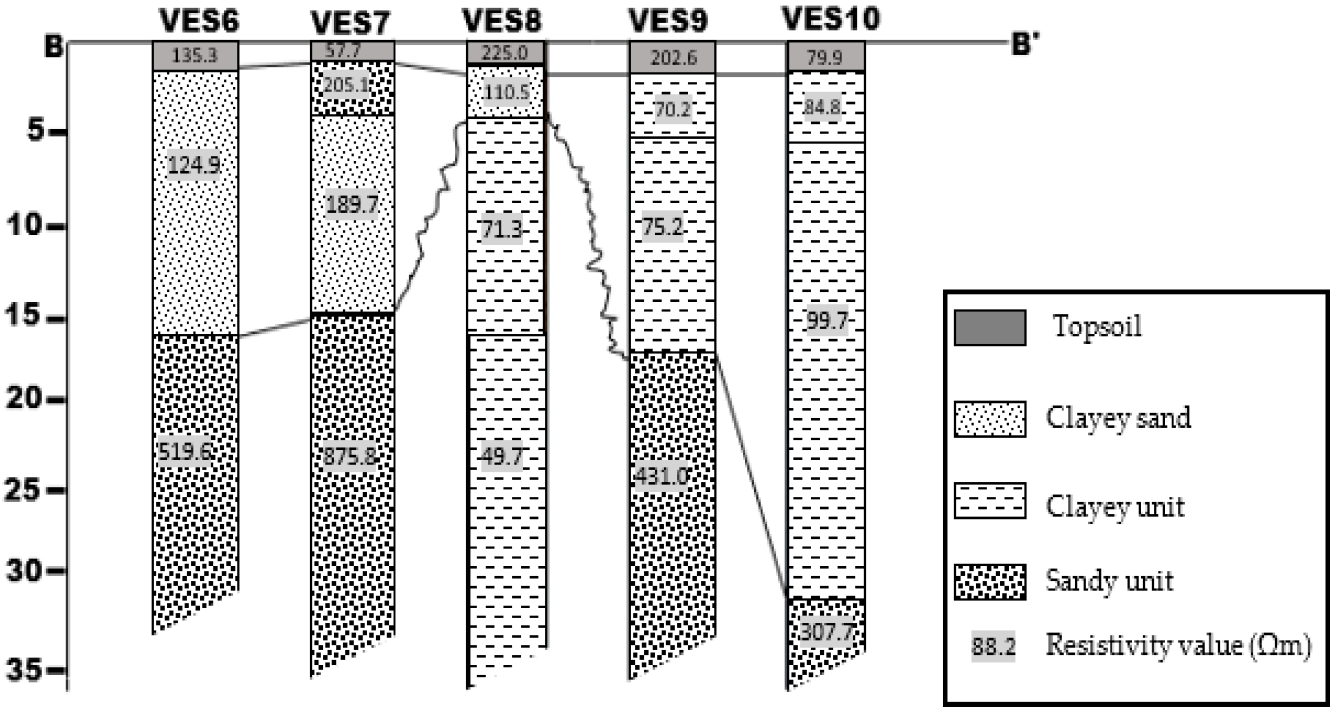

Figure 7. VES-derived geoelectric section from VESs (6–10) with resistivity values in Ohm-m.

The geoelectric parameters of the delineated layers on traverse T3 consist of T3-V11, T3-V12, T3-V13, T3-V14 and T3-V15 (Table 3). The corresponding geoelectric section constructed is presented in Figure 8. Table 3 reveals three to four delineated geoelectric layers:

topsoil, clayey, clayey sand and sandy. The topsoil delineated across all the VESs has resistivity and thickness values that range between 34.7–187.7 Ωm and 0.7–1.1 m, respectively. The second delineated layer in T3-V11 is interpreted to be clayey with resistivity and thickness values of 67.1 Ωm and 11.5 m, respectively. Also, the second geoelectric layer delineated by T3-V12 and T3-V15 is clayey with resistivity and thickness values ranging between 42.0–48.6 Ωm and 8.0–12.1 m, respectively. Also, T3-V13 and T3-V14 have a second geoelectric layer indicative of clayey with resistivity and layer thickness values that range between 27.6–27.8 Ωm and 4.8–16.2 m, respectively. The third stratum beneath T3-V11, T3-V12, T3-V14 and T3-V15 is clayey sand to sandy with a resistivity value that ranges between 143.7–252.5 Ωm. However, the layer thickness could not be determined as this layer is the last delineated geoelectric horizon. However, the delineated third geoelectric layer by T3-V13 is interpreted to be clayey with resistivity and layer thickness values of 72.0 Ωm and 19.4 m. The fourth geoelectric layer by T3-V13 depicts a clayey horizon with a resistivity value of 67.3 Ωm.

Table 3. Geoelectrical parameters of the vertical electrical sounding conducted on traverse T3.

Location	Elevation (m)	Layers	Resistivity (Ωm)	Thickness (m)	Depth (m)	Curve Type	Lithology
T3-V11	56 m	1	187.7	1.1	1.1	H	Topsoil
		2	67.1	11.5	12.6		Clayey
		3	215.9	-	-		Sandy
T3-V12	55 m	1	34.7	1.0	1.0	A	Topsoil
		2	42.0	8.0	9.0		Clayey
		3	252.5	-	-		Sandy
T3-V13	56 m	1	77.6	0.7	0.7	HK	Topsoil
		2	27.8	4.8	5.5		Clayey
		3	72.0	19.4	24.9		Clayey
		4	67.3	-	-		Clayey
T3-V14	57 m	1	91.0	0.9	0.9	H	Topsoil
		2	27.6	16.2	17.1		Clayey
		3	143.7	-	-		Clayey Sand
T3-V15	58 m	1	44.4	1.0	1.0	A	Topsoil
		2	48.6	12.1	13.2		Clayey
		3	227.3	-	-		Sandy

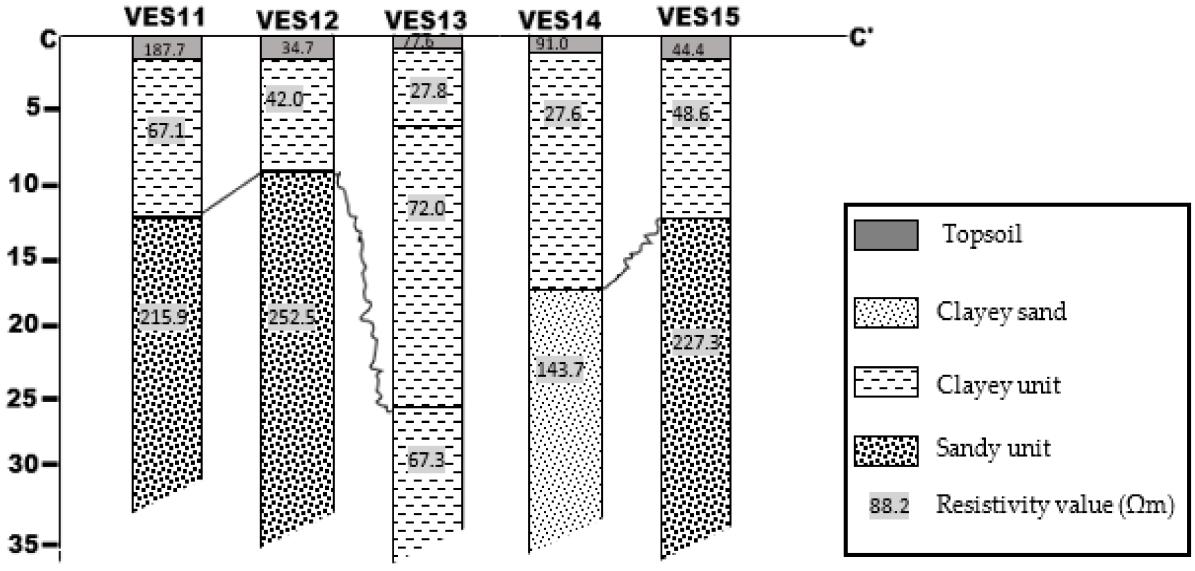

Figure 8. VES-derived geoelectric section from VESs (11–15) with resistivity values in Ohm-m.

Table 4 shows the geoelectric parameters of the delineated geoelectric layers across traverse T4, consisting of V16–20. The corresponding geoelectric section constructed is

presented in Figure 9. Three to four geoelectric layers were delineated: topsoil, clayey, sandy clay, clayey sand, and sand. Generally, the delineated topsoil has resistivity and thickness values ranging from 15.2–212.7 Ωm and 1.0–1.3 m. The second delineated layer along T4-V16 and T4-V17 is clayey with resistivity and layer thickness values ranging from 38.3–56.5 Ωm and 11.9–16.8 m, respectively. However, the second delineated geoelectric layer by T4-V18 is interpreted as clayey with resistivity and layer thickness values of 40.0 Ωm and 12.5 m, respectively. Also, the delineated second layer at T4-V19 and T4-V20 is clayey to clayey sand with resistivity and layer thickness values of 71.4–160.6 Ωm and 2.8–3.1 m, respectively. The third stratum delineated at T4-V16, T4-V17 and T5-V18 is diagnostic of clayey sand to sandy with resistivity values ranging between 174.1–234.7 Ωm. However, the third delineated layer at T4-V19 and T4-V20 is interpreted as clayey with resistivity values ranging from 21.6–29.7 Ωm and a layer thickness of 10.9–17.2 m. The fourth delineated layer by T4-V19 and T4-V20 is the extended clayey unit with resistivity values ranging from 10.3–18.6 Ωm.

Table 4. Geoelectrical parameters of the vertical electrical sounding conducted on traverse T4.

Location	Elevation (m)	Layers	Resistivity (Ωm)	Thickness (m)	Depth (m)	Curve Type	Lithology
T4-V16	57 m	1	85.4	1.0	1.0	Q	Topsoil
		2	71.4	3.1	4.1		Clayey
		3	29.7	17.2	21.3		Clayey
		4	10.3	-	-		Clayey
T4-V17	56 m	1	29.4	1.2	1.2	A	Topsoil
		2	56.5	11.9	13.0		Clayey
		3	234.7	-	-		Sandy
T4-V18	57 m	1	212.7	1.0	1.0	Q	Topsoil
		2	160.6	2.8	3.7		Clayey Sand
		3	21.6	10.9	14.7		Clayey
		4	18.6	-	-		Clayey
T4-V19	56 m	1	107.3	1.2	1.2	H	Topsoil
		2	40.0	12.5	13.7		Clayey
		3	190.8	-	-		Clayey Sand
T4-V20	58 m	1	15.2	1.3	1.3	A	Topsoil
		2	38.3	16.8	18.1		Clayey
		3	174.1	-	-		Clayey Sand

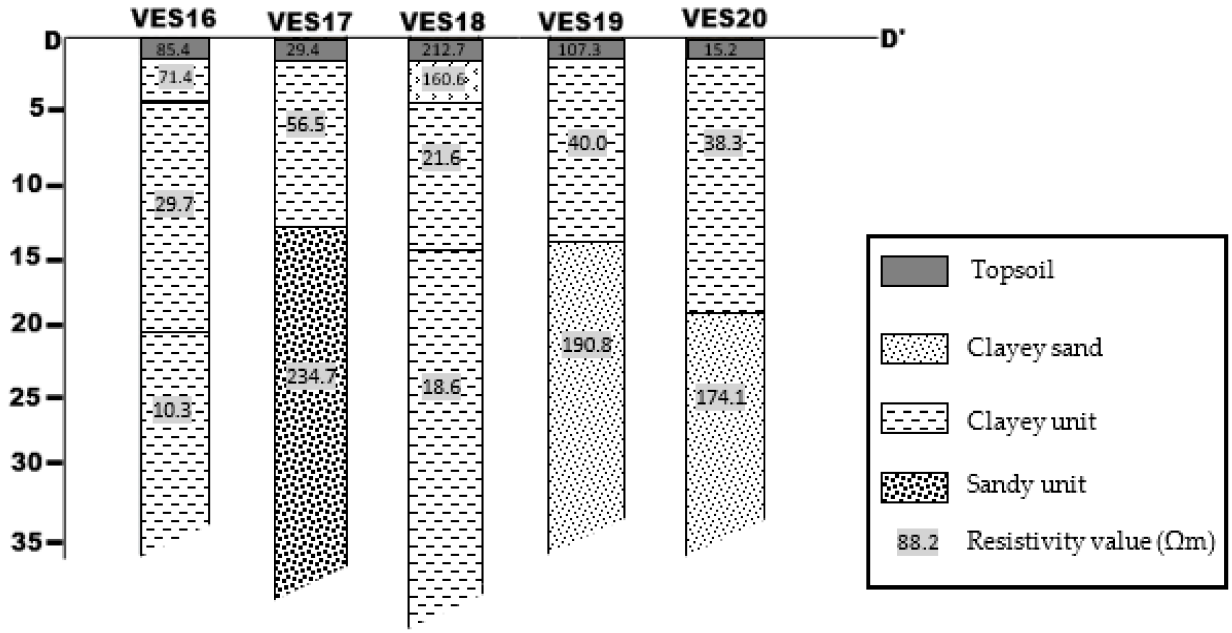

Figure 9. VES-derived geoelectric section from VESs (16–20) with resistivity values in Ohm-m.

4.2. 2D Resistivity Imaging

The results of 2D electrical resistivity imaging are presented in Figures 10–13. The inversion models reveal geoelectric layers similar to those observed in the sounding results. The inverted resistivity model for Traverse T1 (Figure 10) shows resistivity values ranging from 11–544 Ωm with a depth of penetration of up to 50 m. Four geoelectric layers are mappable in the inverted model, including topsoil, clayey, sandy, and compacted sand units across the profile. The topsoil is comprised of compacted sand mixed with lateritic clay. The clay units are of two types; wet clay with resistivity values of less than 31 Ωm occurs as lenses at about 10–15 m depth at the central portion of the traverse, while the second type of clay occurs at a deeper depth of about 18 m downwards. A clayey unit with resistivity values of 31–60 Ωm occurs laterally about 100 m between the horizontal distance of 40 m and 140 m across the profile. The clayey unit also occurs between 5 m and 35 m depths, enclosing the wet clay units within the subsurface. This clayey unit forms a perched aquifer in the subsurface.

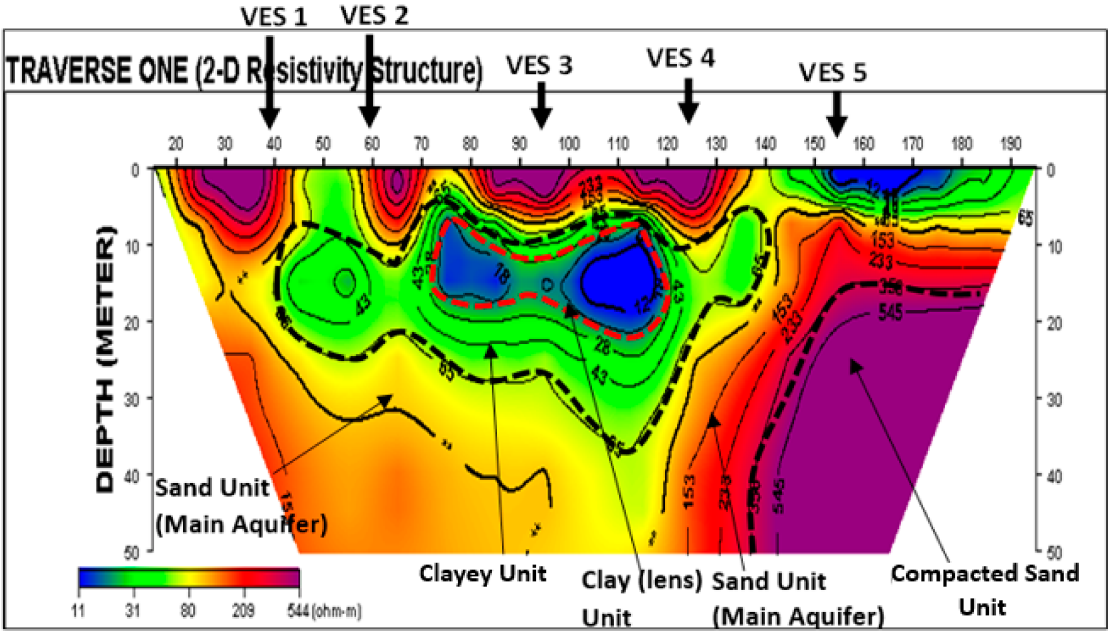

Figure 10. 2D inverse resistivity model for traverse T1.

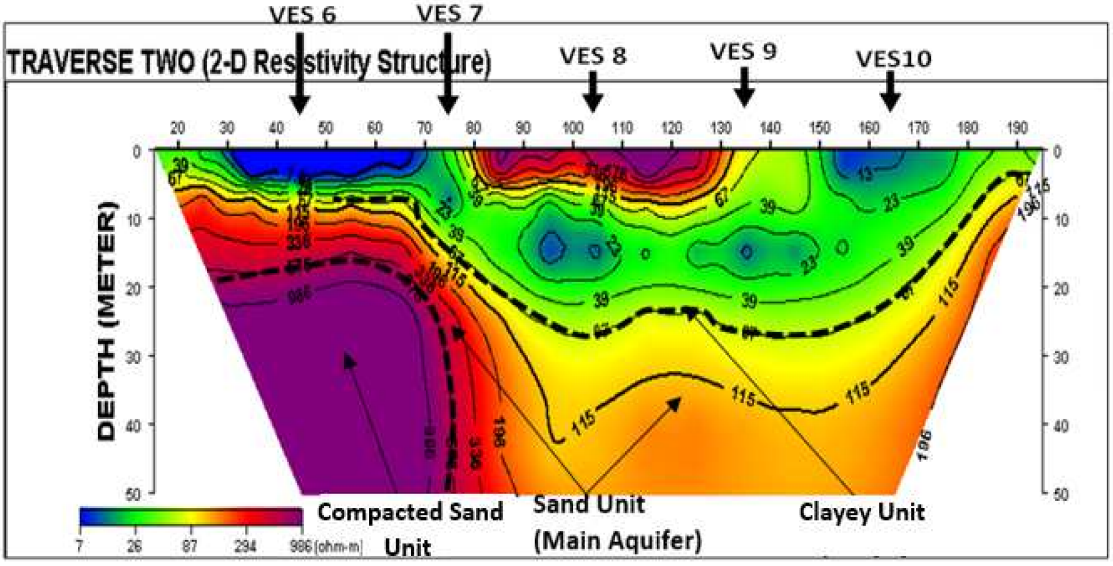

Figure 11. 2D inverse resistivity model for traverse T2.

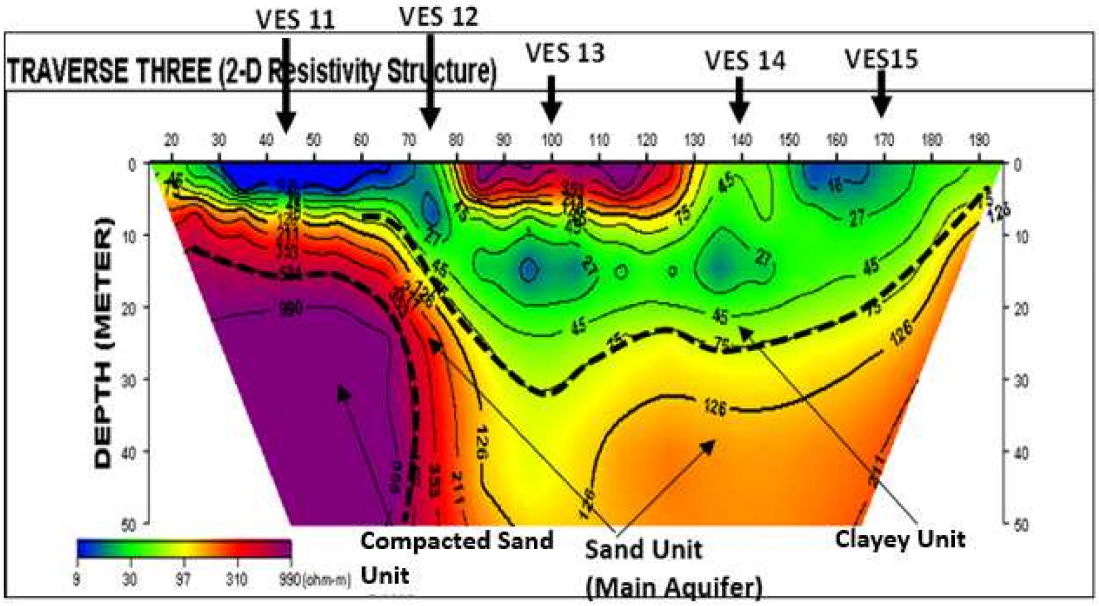

Figure 12. 2D inverse resistivity model for traverse T3.

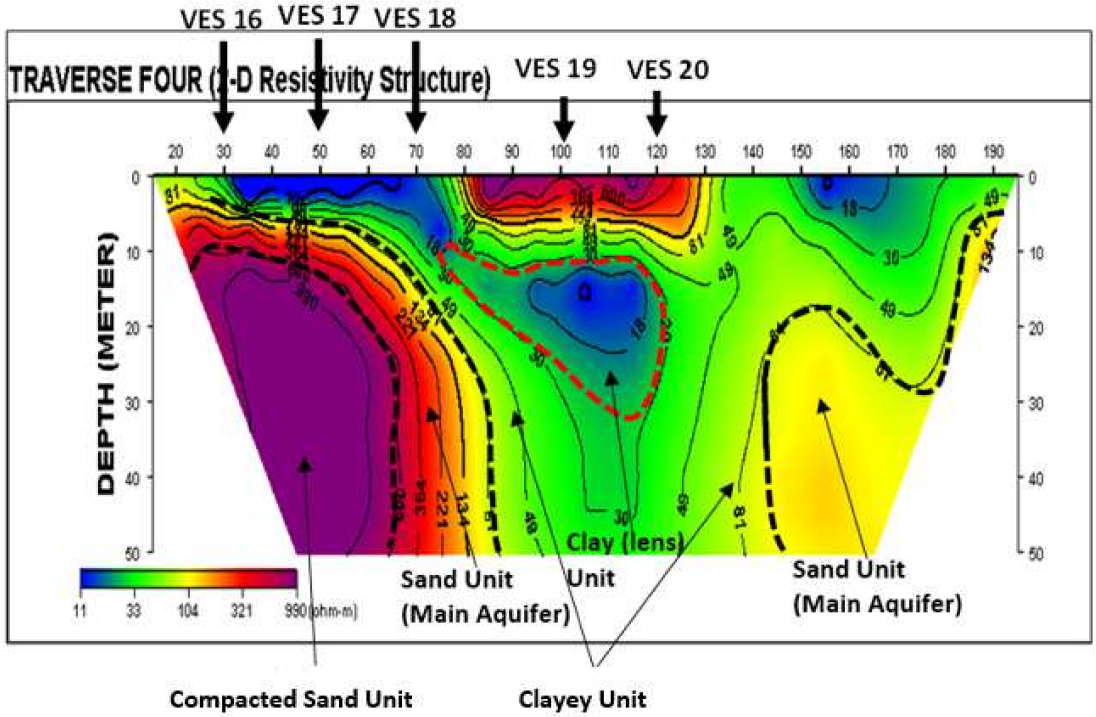

Figure 13. 2D inverse resistivity model for traverse T4.

Figure 11 shows the inversion model for Traverse T2 with resistivity ranges of 7–986 Ωm. The interpretive geoelectric layers include the topsoil comprising reworked sand and clay intercalations. A clayey section with resistivity values of 15–80 Ωm occurs from the surface to about 25 m depth. This unit enclosed some pockets of clay lenses with resistivity values of 7–15 Ωm at about 12–13 m within the electrode positions 40 and 150 across the profile. A third geoelectric layer is a clayey to sandy unit with resistivity values 87–294 Ωm occurring at a depth of 10–20 m from the origin to 75 m along the traverse and a depth of 20–50 m from the horizontal distance of 75 m to 200 m across the profile. A laterally extensive thick compacted sandy unit with resistivity values greater than 300 Ωm occurs at a depth of 20 m downwards from the origin of the traverse line to 75 m.

The inverted resistivity model for Traverse T3 is presented in Figure 12, with resistivity values 9–990 Ωm. The delineated geoelectric layers are interpreted to include topsoil, clayey, sandy, and compacted sandy units. The topsoil consists of the intercalation of sand and clay units that have become compacted due to the human activities in the area. The clayey unit has resistivity values of 30–90 Ωm, with the depth of occurrence ranging from 5 m from the traverse inception to 30 m at the center portion to the 5 m at the end of the profile line. The geoelectric unit envelops several pockets of wet clay units with resistivity values of 9–18 Ωm. The sandy unit occurs at a depth range of 5–15 m from the inception of the profile line to about 75 m, while it occurs down to the depth of 50 m from the horizontal distance of 75 m to 200 m on the traverse. Pockets of clay units appear from a depth of about 15 m to 50 m between 0–75 electrode positions across the profile line. Figure 13 shows the inversion model for traverse T4, with resistivity ranges of 11–990 Ωm. The interpretive geoelectric layers include the topsoil comprising reworked sand and clay intercalations. Pockets of wet clay lenses with resistivity values 11–23 Ωm occur close to the surface and at the profile line's central portion. There is an occurrence of a clayey layer with resistivity values of 23–100 Ωm with depths of about 5 m at the origin of the traverse, 50 m at the central portion and about 5 m depth at the end of their profile line. A third geoelectric layer was delineated as a clayey sand to sandy unit with resistivity values of 104–321 Ωm, occurring between the depth of 5–10 m from the origin to 75 m along the traverse. This same sand unit occurs again at 140–180 m along the traverse from the depth of 20 m downwards. A laterally extensive thick compacted sandy unit with resistivity values greater than 400 Ωm also occurs at a depth of 10 m downwards from the origin of the traverse line to about 75 m.

5. Discussion

The 2D electrical resistivity imaging and resistivity soundings were integrated to characterize the subsurface. Electrical resistivity properties of the subsurface geology depend significantly on permeability, porosity, degree of water saturation, fluid chemical composition, and clay content. The electrical resistivity of a geologic formation decreases as porosity, water saturation, and permeability increase. The presence of clay minerals in a water-bearing rock formation increases the conductivity of the rock formation through the ion exchange process [51]. The delineated geoelectric layers, including topsoil, clayey, compacted and unconsolidated sandy units, were present in all the traverses, as revealed by the 2D resistivity images. The topsoil consists of reworked unconsolidated sand–clay intercalations. The clay unit occurred in two forms: a wet clay unit closer to the surface and formed pockets of clay lenses across the study area. The compacted sandy unit delineated along the profile was extensive. The third delineated geoelectric layer is a mixture of clayey and clayey sand, which appears as clayey sand in some interpretive sounding curves in the study area. The fourth delineated geoelectric layer is an unconsolidated sand unit present across the entire study area. The sand unit is a coastal plain sand, a mixture of alluvium and Benin continental sand Formation.

The initial hydrogeological conceptual models for each survey traverse were developed, showing the two-dimensional distribution of the mapped two aquiferous units in the area (Figures 14–17). The interpreted clayey sand and clayey units are the shallow, unconfined low-yield aquifer, or aquitard. This shallow aquiferous unit is believed to have a low yield due to its high clay content, which will reduce its permeability, thereby reducing the fluid flow through the unit. This shallow aquifer (aquitard) seems to occur along all the traverse lines and is believed to have low productivity due to poor transmissivity and low yield [52,53]. The aquifer's productivity and yield depend on its porosity, permeability, and transmissivity, which are related to the clay, shale, and silt volume within its formation [52–55]. The results of the sounding curves showed the thicknesses of the shallow, low-yield aquifer to range from 15.5–18.8 m, 11.5–25.4 m, 8.0–19.4 m, 3.1–16.8 m for traverse T1, T2, T3 and T4, respectively. This shallow aquifer comprised sand, silt, and clay units of the continental plain sand of the Benin Formation [39,40] (Figure 2). The 2D resistivity images revealed that this layer is thickened within the central portion of traverses

T1–T4, enclosing a clay lens unit and forming a perched aquifer within the study area. This shallow unconfined aquifer may be prone to pollution from industrial effluents and seawater incursions based on its much shallower depth of occurrence [24–26,36,37,43,56–60]. The high-yield main aquifer is the delineated unconsolidated sand unit. The resistivity soundings revealed the depth to the top of this coastal plain sand unit as 1.0–20.1 m, 0.7–30.4 m, 12.6 m to 17.1 m and 13.0 m to 18.1 m on traverses T1, T2, T3 and T4, respectively. 2D resistivity images revealed the presence of the high-yield main aquifer across all the traverses. The interpreted deeper main aquifer is the beach sand unit of the Tertiary alluvium deposits within the Dahomey Basin [39,40] (Figure 2). The compacted sand at the base confines the main aquifer, while the clayey sand and clayey unit confine it at the top.

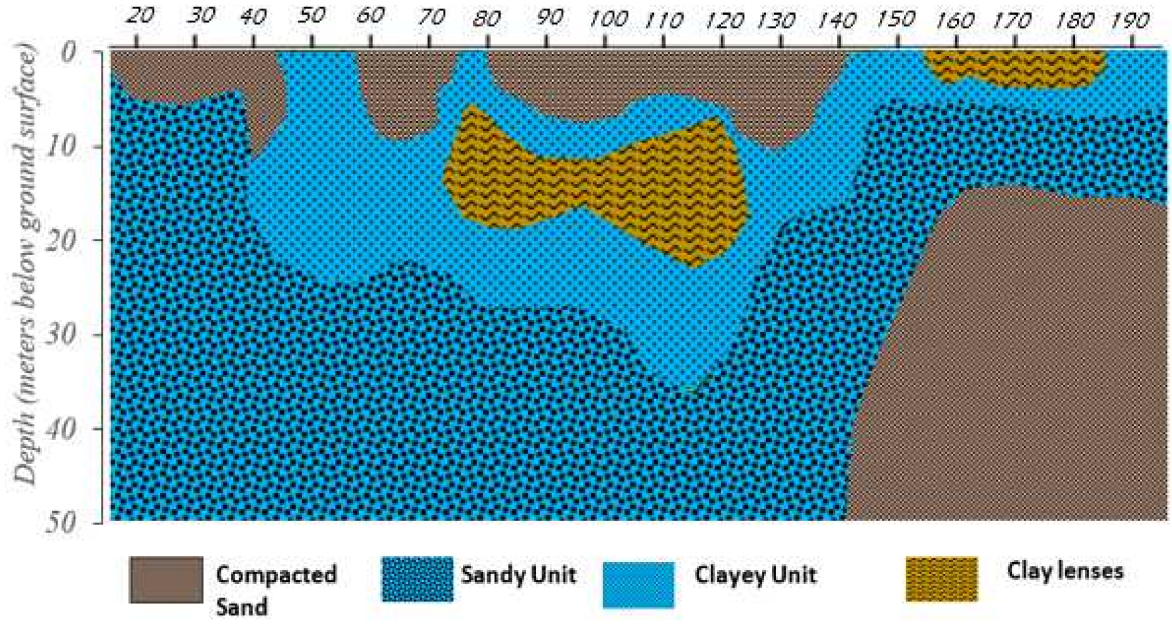

Figure 14. 2D initial hydrogeological conceptual model for traverse T1.

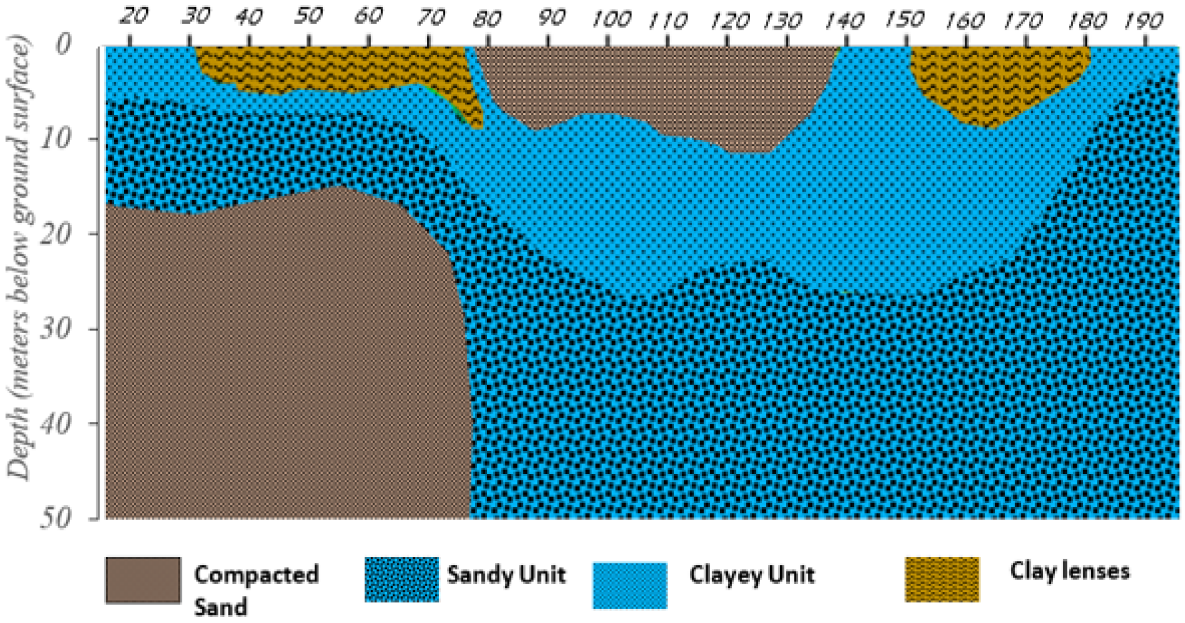

Figure 15. 2D initial hydrogeological conceptual model for traverse T2.

Figure 18 shows the 3D distribution of the geoelectric sections with depth. Along the study area's northern, central and southern parts, the clay sequence acts as the perched

aquifer. At the western end, there is a pocket clayey unit grading into a sandy horizon; the clay horizon stretches from the surface to the investigated depth. The impervious unit (clay) protects the groundwater-bearing unit (sand) by acting as the aquitard; thus, it impedes the direct flow of surficial water percolating into the groundwater system. The groundwater is confined within the geoelectric sequences. Figure 19 revealed the lithologic units from the direct observation of the borehole drilled cuttings. The major lithology is the sandy materials with varying sizes. The lateritic unit (impervious) is the overlying section. Beneath this unit are different sandy horizons permitting the transmission of the groundwater; they are underlain by clayey sand horizons preventing further groundwater infiltration. These impervious units (laterite and clayey sand) confine the groundwater within the study area. Generally, there is an agreement between the deductions obtained from the geoelectric sequence and the borehole lithologic units in establishing that the aquifer unit within the area is confined.

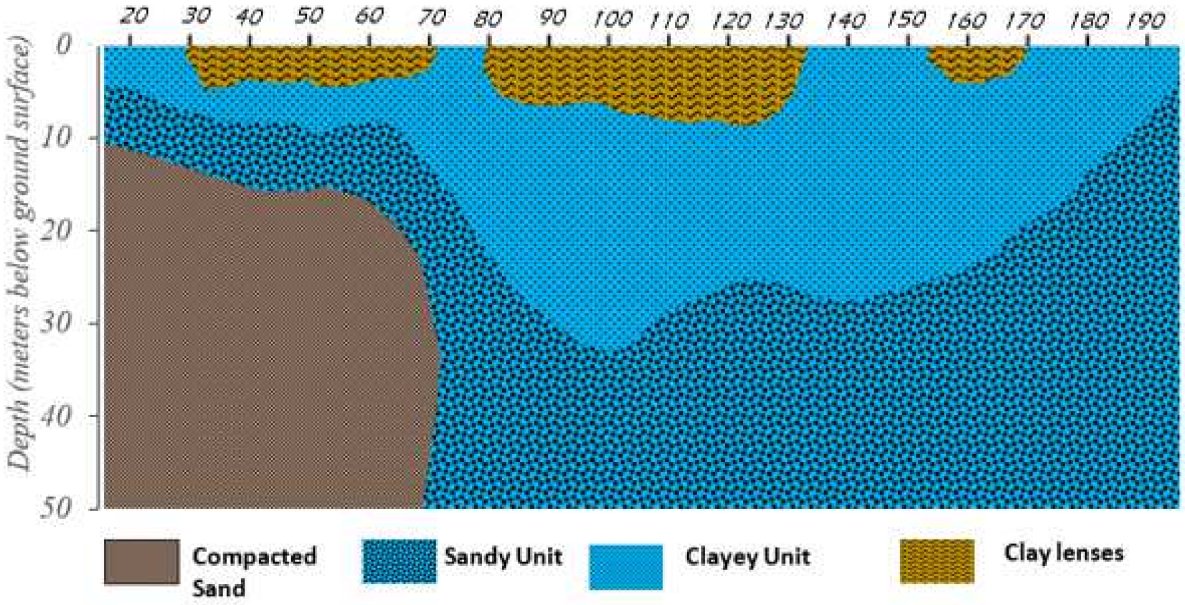

Figure 16. 2D initial hydrogeological conceptual model for traverse T3.

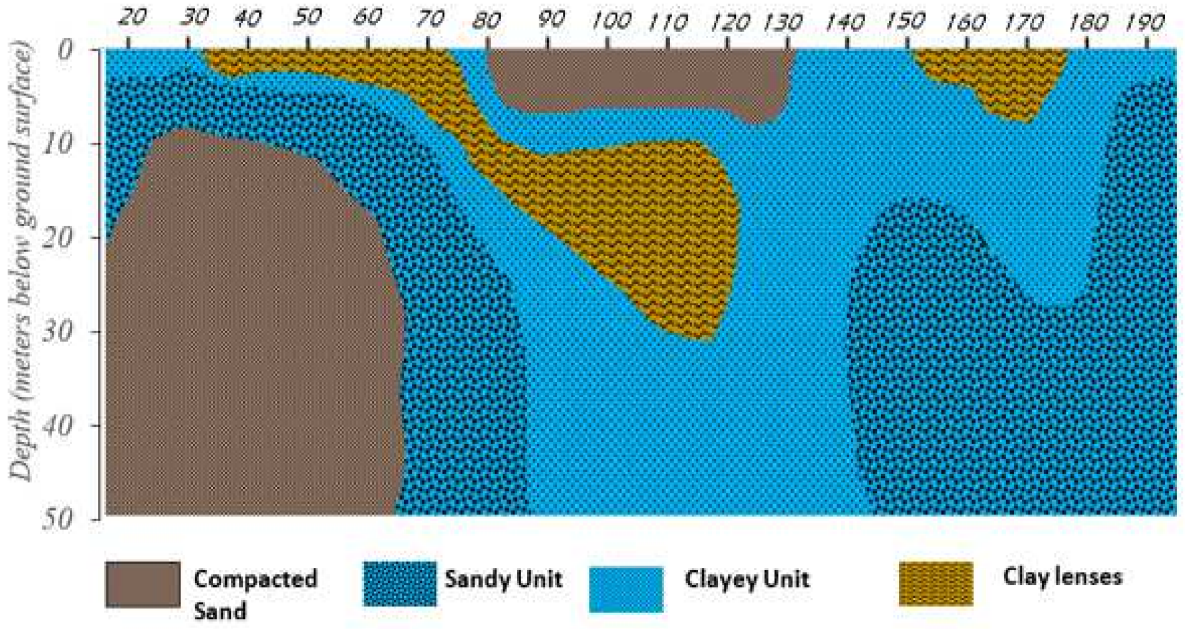

Figure 17. 2D initial hydrogeological conceptual model for traverse T4.

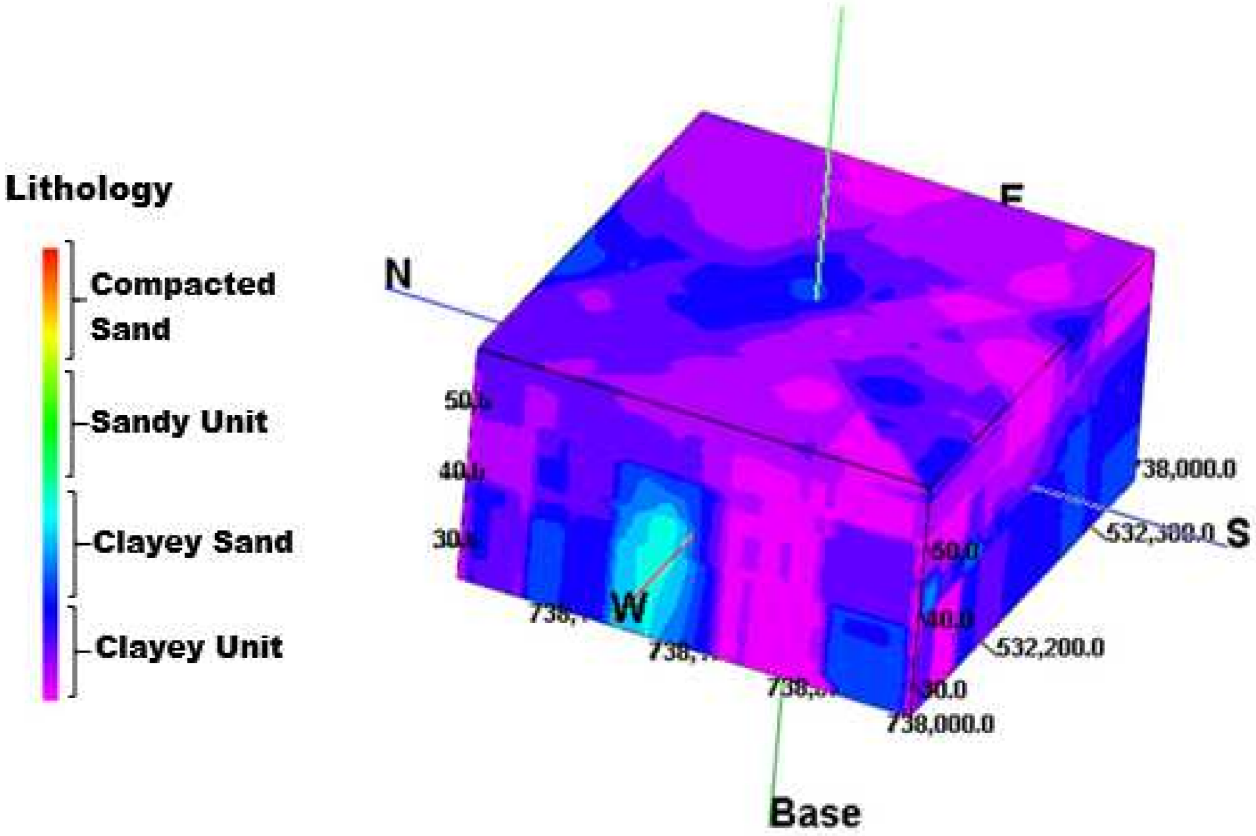

Figure 18. 3D lithologic modeling from the VES data.

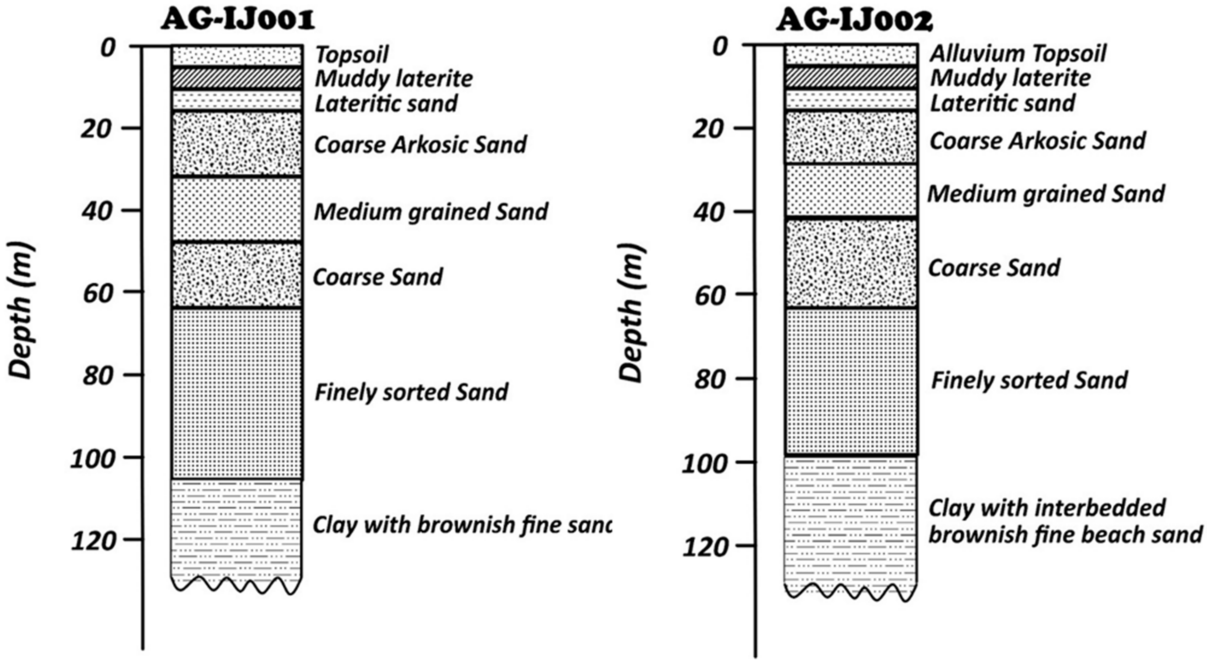

Figure 19. Borehole logs showing lithologic units from the study area.

It is recommended that the main aquifer within the area should be the target for efficient groundwater extraction due to its high yield. It is equally recommended that an adequate hydrogeophysical report from the experts should be required before digging any borehole in Lagos, Southwestern Nigeria. This will forestall cases of drilling into the polluted aquifer and indiscriminate drilling of boreholes that can lead to land subsidence

and building collapse. Despite the crucial role of groundwater for domestic, industrial and agricultural use and sustainability of the ecosystem, many studies have revealed the empirical relationship between groundwater overexploitation and land subsidence in many urban cities across the world [61–69]. There is a need for the Lagos state government to come up with regulation standards for getting approval and licenses for digging boreholes and the volume of water that could be abstracted from these natural resources. Land subsidence, the gradual sinking or settling of the earth's surface, can result from various causes, including excessive groundwater withdrawal [61–69]. Land subsidence has caused severe damage to infrastructure and the environment, making it a serious issue that needs to be prevented by the government of Lagos. One of the most serious impacts of the overexploitation of groundwater on land subsidence is the reduced volume of water within the aquifer, causing it to collapse, leading to subsidence [63,65,67–69]. When an aquifer is depleted, it can no longer support the weight of the land above it, causing it to sink or settle. This can damage roads, buildings and other structures, causing erosion, increased flooding and loss of agricultural land. Also, the overexploitation of groundwater can result in soil and water resource salinization [2,6,7,20,24,37]. When too much water is pumped from the aquifer, the water table can drop, bringing saltwater from deeper layers up to the surface [2,24,37]. This can cause soil and water salinization, making the soil and water less productive and affecting agriculture, wildlife, and human health [2,6,7,20,24,37]. To prevent all these hazardous impacts of overexploitation of groundwater in Lagos, it is important for the Lagos state government to implement sustainable groundwater management practices. These include implementing standard regulations for managing groundwater pumping and monitoring the water table across the entire Lagos state. While groundwater continues to be a valuable and indispensable natural resource for human survival, its exploitation should be done in a responsible and sustainable manner to protect the environment and ensure the long-term health and well-being of communities and ecosystems.

The findings of this research serve as a baseline for groundwater resource management within the coastal areas of Lagos. Before developing groundwater resources, it is pertinent to understand the subsurface geology and groundwater potential. The data and the information obtained from this study provide information on the groundwater potential of the coastal areas in Lagos. They are vital for siting both boreholes and hand-dug wells in these typical coastal aquifers. The aquifers' vulnerability to pollution and the development of protective measures relies largely on understanding aquifer lithology. In this case, the shallow aquifer is typically unconfined and, therefore, vulnerable to surface pollution compared to the deeper aquifer. Due to unconfinement conditions, the shallow aquifer also has great direct recharge potential. Sustainable development and management of groundwater resources require a good understanding of the groundwater potential and the vulnerability of aquifers to pollution and recharge potential, among other factors. While this study is on a local scale, the application of the findings would be wide in many coastal areas that exhibit similar geology.

6. Conclusions

This research focuses on applying geoelectrical resistivity imaging to assess the groundwater potential of the coastal aquifer. Resistivity soundings were integrated with 2D electrical resistivity imaging to evaluate the subsurface layered media and their corresponding geoelectric parameters, such as average electrical resistivities and thicknesses. The delineated geoelectric layers include topsoil, clayey, compacted, and unconsolidated sand. Two aquiferous units were mapped in the area due to their clay content. The first is a shallow, low-yield aquifer, the delineated clayey/clayey sand unit. The shallow aquifer unit is the continental plain sand of the Benin Formation. The electrical resistivity values and depth to the top of this aquiferous zone are 65–190 Ωm and 0.8−5.5 m, respectively, which is considered clayey/clayey sand. However, this shallow aquifer is prone to several pollutions from industrial effluents and seawater intrusion. The second aquifer is clay-free, unconsolidated beach sand, adjudged to be of the Tertiary alluvium deposits. The electrical

resistivity values and depth to the top of this main aquifer system are 176–520 Ωm and 0.7–30.4 m. The lateral variability and distribution of the geoelectrical layers are revealed in 2D geoelectrical resistivity images. The study has confirmed that the results of 2D electrical resistivity imaging complement those of the electrical soundings in groundwater resource evaluation within a coastal environment. Pumping tests are recommended to evaluate the hydraulic parameters of the two delineated aquifer units in the area. The geoelectrical resistivity technique can resolve groundwater-related challenges involving identifying groundwater-bearing units and establishing the nature of the aquifer unit. It has also revealed that the perched aquifer and the main aquifer unit could be delineated using the geophysical technique, which in turn aids the siting of either tube wells or boreholes for groundwater extraction. The findings of this research are essential for groundwater resource sustainability in Lagos, Nigeria. Since understanding subsurface geology is essential for successful groundwater resource extraction, there is a need for a viable policy restricting unprofessional borehole drillers with little-to-no knowledge of earth sciences in Lagos. Also, there is a need to implement a policy regulating groundwater abstraction in Lagos to ensure its management and sustainability.

Author Contributions: Conceptualization, K.D.O., M.M. and M.G.; methodology, K.D.O., O.J.R., P.O.F. and J.A.-J.; investigation, K.D.O., O.J.R., J.A.-J., A.A.O., B.D., P.O.F. and M.G.; writing—original draft preparation, K.D.O.; writing—review and editing, M.M., A.A.O., B.D. and M.G.; funding acquisition, M.M. and K.D.O. All authors have read and agreed to the published version of the manuscript.

Funding: This work was funded by the Research Supporting Project number (RSP2023R89), King Saud University, Riyadh, Saudi Arabia.

Institutional Review Board Statement: Not applicable.

Informed Consent Statement: Not applicable.

Data Availability Statement: The data is available upon request from the corresponding author.

Acknowledgments: The authors would like to thank the Research Supporting Project number (RSP2023R89), King Saud University, Riyadh, Saudi Arabia, for funding this work.

Conflicts of Interest: The authors declare no conflict of interest.

References

1. Emordi, E.C.; Osiki, O.M. Lagos: The 'Vigilized' city. *Inf. Soc. Justice* **2008**, *2*, 95–109.
2. Aladejana, J.A.; Kalin, R.M.; Sentenac, P.; Hassan, I. Hydrostratigraphic characterization of shallow coastal aquifer of Eastern Basin, S/W Nigeria, using integrated hydrogeophysical approach; implications for saltwater intrusions. *Geosciences* **2020**, *10*, 65. [CrossRef]
3. Urish, D.W.; Frohlich, R.K. Surface Electrical Resistivity in Coastal Groundwater Exploration. *Geoexploration* **1990**, *26*, 267–289. [CrossRef]
4. Sajeena, S.; Hakkim, A.; Kurien, V.M.E.K. Identification of groundwater prospective zones using geoelectrical and electromagnetic surveys. *Int. J. Eng. Invent.* **2014**, *3*, 17–21.
5. Ogunba, A. Sustainable groundwater management in Lagos, Nigeria: The regulatory framework. *Afr. Focus* **2015**, *28*, 146–155. [CrossRef]
6. Olanrewaju, D. Soak-away systems and possible groundwater pollution problems in developing countries. *Perspect. Public Health* **1990**, *110*, 108–112. [CrossRef]
7. Balogun, I.I.; Akoteyon, I.S.; Soneye, A. Seasoned-induced variation in water table depth and selected chemical parameters of groundwater in Lagos coastal plain sand aquifer, Nigeria. *J. Appl. Sci. Environ. Manag.* **2019**, *23*, 1465–1473.
8. Ikuemonisan, F.E.; Ozebo, V.C.; Olatinsu, O.B. Investigating and modelling ground settlement response to groundwater dynamic variation in parts of Lagos using space-based retrievals. *Solid Earth Sci.* **2021**, *6*, 95–110. [CrossRef]
9. Adetoyinbo, A.A.; Adelegan, F.T.; Bello, A.K. Environmental impact assessment of the portability of water from borehole, hand dug well and stream at Itagunmodi gold deposits Southwestern Nigeria using FORTRAN algorithm for monitoring leachates and interpreting physiochemical data of contaminants in groundwater. *Int. J. Water Res. Environ. Eng.* **2015**, *7*, 1–6.
10. Danert, K.; Healy, A. Monitoring groundwater use a domestic water source by urban household: Analysis of data from Lagos state, Nigeria and sub-Saharan Africa with implications for policy and practice. *Water* **2021**, *13*, 568. [CrossRef]

11. Healy, A.; Upton, K.; Capstick, S.; Bristow, G.; Tijani, M.; MacDonald, A.; Goni, I.; Bukar, Y.; Whitmarsh, I.; Theis, S.; et al. Domestic groundwater abstraction in Lagos, Nigeria: A disjuncture in the science-policy-practice interface? *Environ. Res. Lett.* **2020**, *15*, 045006. [CrossRef]
12. Alley, W.M.; Reilly, T.E.; Franke, O.L. Sustainability of Groundwater Resources. *US Geol. Surv. Circ.* **1999**, *1186*, 79.
13. Carrasquilla, A.; Gonçalves, C.A.; Ulugergerli, E. Evaluating the Performance of Different Geophysical Methods for Groundwater Prospecting in Espirito Santo Basin—Southeast Brazil. *Tecnociencia* **2007**, *9*, 89–106.
14. Metwaly, M.; Elawadi, E.; Sayed, S.R.M.; AlFouzan, F.; Mogren, S.; Arifi, N. Groundwater exploration using geoelectrical resistivity technique at Al-Quwy'yia area central Saudi Arabia. *Int. J. Phys. Sci.* **2012**, *7*, 317–326. [CrossRef]
15. Metwaly, M.; AlFouzan, F. Application of 2-D geoelectrical resistivity tomography for subsurface cavity detection in the eastern part of Saudi. *Arab. Geosci. Front.* **2013**, *4*, 469–476. [CrossRef]
16. Singh, K.K.K. Delineation of waterlogged area in inaccessible underground workings at Hingir Rampur Colliery using 2D Resistivity imaging: A case study. *Bull. Engr. Geol. Environ.* **2013**, *72*, 115–118. [CrossRef]
17. Aizebeokhai, A.P.; Oyeyemi, K.D.; Joel, E.S. Groundwater potential assessment in a sedimentary terrain, southwestern Nigeria. *Arab. J. Geosci.* **2016**, *9*, 496–511. [CrossRef]
18. Khalid, M.I.; Didar-UIIslam, S.M.; Uddin, M.J.; Majunder, R.K. Coastal groundwater characterization from geoelectrical measurements. A case study at Kalapara, Patuakhalil, Bangladesh. *J. Appl. Geol.* **2020**, *5*, 112.
19. Yusuf, M.A.; Abiye, T.A. Risks of groundwater pollution in coastal areas of Lagos, southwestern Nigeria. *Groundw. Sustain. Dev.* **2019**, *9*, 100222. [CrossRef]
20. Al-sayed, E.A.; EL-Qady, G.; Soliman, N. Groundwater exploration and mapping the seawater intrusion at Matruh area, North coast, Egypt. *Int. J. Water Resour. Arid. Environ.* **2017**, *6*, 115–125.
21. Sanddeep, K.; Reethu, M. Geoelectrical and hydrochemical characteristics of shallow lateritic aquifer in southwestern India. *Geosystems Geoenvironment* **2023**, *2*, 100147. [CrossRef]
22. Ige, O.O.; Obasaju, D.O.; Baiyegunhi, C.; Ogunsanwo, O.; Baiyegunhi, T.L. Evaluation of aquifer hydraulic characteristics using geoelectrical sounding, pumping and laboratory tests: A case study of Lokoja and Patti Formations, Southern Bida Basin, Nigeria. *Open Geosci.* **2018**, *10*, 807–820. [CrossRef]
23. Obiora, D.N.; Onwuka, O.S. Groundwater Exploration in Ikorodu, Lagos-Nigeria: A Surface Geophysical Survey Contribution. *Pacific J. Sci. Technol.* **2005**, *6*, 86–93.
24. Adepelumi, A.A.; Ako, B.D.; Ajayi, T.R.; Afolabi, O.; Omotoso, E.J. Delineation of saltwater intrusion into the freshwater aquifer of Lekki Peninsula, Lagos. *Niger. J. Environ. Geol.* **2008**, *56*, 927–933. [CrossRef]
25. Oyedele, K.F.; Oladele, S. Geoelectrical assessment of groundwater potential in the coastal aquifer of Lagos, Nigeria. In *Advances in the Research of Aquatic Environments*; Lambrakis, N., Stournaras, G., Katsanou, K., Eds.; Springer: Berlin/Heidelberg, Germany, 2011; Volume 2, pp. 29–33. [CrossRef]
26. Oyedele, K.F.; Ayolabi, E.A.; Adeoti, L.; Adegbola, R.B. Geophysical and hydrogeological evaluation of rising groundwater level in the coastal areas of Lagos. *Bull. Eng. Geol.* **2009**, *68*, 137–143. [CrossRef]
27. Aizebeokhai, A.P.; Oyeyemi, K.D. Application of geoelectrical resistivity imaging and VLF-EM for subsurface characterization in a sedimentary terrain, Southwestern Nigeria. *Arab. J. Geosci.* **2014**, *8*, 4083–4099. [CrossRef]
28. Aizebeokhai, A.P.; Oyeyemi, K.D. The use of the multiple-gradient array for geoelectrical resistivity and induced polarization imaging. *J. Appl. Geophys.* **2014**, *111*, 364–376. [CrossRef]
29. Ameloko, A.A.; Ayolabi, E.A.; Adewale, A. Time dependent electrical tomography and seasonal variation assessment of groundwater around Olushosun dumpsite Lagos, South-west Nigeria. *J. Afr. Earth Sci.* **2018**, *147*, 243–253.
30. Jekayinfa, S.M.; Oladunjoye, M.A.; Doro, K.O. Imaging the distribution of bitumen contaminants in shallow coastal plain sands in southwestern Nigeria using electrical resistivity. *Environ. Earth Sci.* **2023**, *82*, 55. [CrossRef]
31. Aizebeokhai, A.P.; Oyeyemi, K.D. Geoelectrical characterization of basement aquifers: The case of Iberekodo, southwestern Nigeria. *Hydrogeol. J.* **2017**, *26*, 651–664. [CrossRef]
32. Aizebeokhai, A.P.; Ogungbade, O.; Oyeyemi, K.D. Integrating VES and 2D ERI for near surface characterization in a crystalline basement terrain. In *SEG Technical Program Expanded Abstract*; Society of Exploration Geophysicists: Houston, TX, USA, 2017. [CrossRef]
33. Aizebeokhai, A.P.; Ogungbade, O.; Oyeyemi, K.D. Application of geoelectrical resistivity for delineating crystalline basement aquifers in Basiri, Ado-Ekiti, Southwestern Nigeria. *Arab. J. Geosci.* **2021**, *14*, 51. [CrossRef]
34. Ganiyu, S.A.; Badmus, B.S.; Oladunjoye, M.A.; Aizebeokhai, A.P.; Ozebo, V.C.; Idowu, O.A.; Olurin, O.T. Assessment of groundwater contamination around active dumpsite in Ibadan southwestern Nigeria using integrated electrical resistivity and hydrochemical methods. *Environ. Earth Sci.* **2016**, *75*, 643. [CrossRef]
35. Doro, K.O.; Adegboyega, C.O.; Aizebeokhai, A.P.; Oladunjoye, M.A. The Ibadan Hydrogeophysics Research Site (IHRS)—An Observatory for Studying Hydrological Heterogeneities in A Crystalline Basement Aquifer in Southwestern Nigeria. *Water* **2023**, *15*, 433. [CrossRef]
36. Akintunde, O.A.; Ozebo, C.V.; Oyedele, K.F. Triangulation approach for mapping groundwater suitability zones in coastal areas around Lagos, Nigeria. Using multi-criteria decision-making technique. *NRIAG J. Astron. Geophys.* **2021**, *10*, 423–442. [CrossRef]
37. Akintunde, O.A.; Ozebo, C.V.; Oyedele, K.F. Groundwater Quality around upstream and downstream area of Lagos Lagoon using GIS and Multispectral analysis. *Sci. Afr.* **2022**, *16*, e01126. [CrossRef]

38. Ojo, O. Rainfall Trends in West Africa, 1901–1985; the influence of climate change and climate variability on the hydrologic regime and water resources. *IAHS Publ.* **1987**, *168*, 37–42.
39. Oke, S.A.; Vermeulen, D.; Gomo, M. Aquifer vulnerability assessment of the Dahomey Basin, using the RTT method. *Environ. Earth Sci.* **2016**, *75*, 964–973. [CrossRef]
40. Omatsola, M.E.; Adegoke, O.S. Tectonic evolution of the Cretaceous stratigraphy of the Dahomey Basin. *J. Min. Geol.* **1981**, *15*, 78–83.
41. Olabode, S.O. Siliciclastic slope deposits from the Cretaceous Abeokuta Group, Dahomey (Benin) Basin, Southwestern Nigeria. *J. Afr. Earth Sci.* **2006**, *46*, 187–200. [CrossRef]
42. Obaje, N.G. Geology and mineral resources of Nigeria. In *Lecture Notes in Earth Sciences*; Brooklyn, S.B., Bonn, H.J.N., Gottingen, J.R., Graz, K.S., Eds.; Springer: Berlin/Heidelberg, Germany, 2009. [CrossRef]
43. Adegoke, O.S. Eocene stratigraphy of Southern Nigeria. *Bur. Rech. Geol. Min. Mem.* **1969**, *69*, 23–47.
44. Edwards, L.S. A modified pseudosection for resistivity and induced polarization. *Geophysics* **1977**, *42*, 1020–1036. [CrossRef]
45. Dahlin, T.; Loke, M.H. Resolution of 2D Wenner resistivity imaging as assessed by numerical modelling. *J. Geophys.* **1998**, *38*, 237–249. [CrossRef]
46. Olayinka, A.I.; Yaramanci, U. Assessment of the reliability of 2D inversion of apparent resistivity data. *Geophys. Prospect.* **2000**, *48*, 293–316. [CrossRef]
47. Dahlin, T.; Zhou, B. A numerical comparison of 2D resistivity imaging with 10 eletrode arrays. *Geophys. Prospect.* **2004**, *52*, 379–398. [CrossRef]
48. Neyamadpour, A.; Wan Abdullah, W.A.T.; Taib, S. Use of four-electrode arrays in three-dimensional electrical resistivity imaging survey. *Stud. Geophys. Geod.* **2009**, *53*, 389–402. [CrossRef]
49. Okpoli, C.E. Sensitivity and resolution capacity of electrode configurations. *Int. J. Geophys.* **2013**, *2013*, 608037. [CrossRef]
50. Yi, M.J.; Kim, J.H.; Chung, S.H. Enhancing the resolving power of least-squares inversion with active constraints balancing. *Geophysics* **2003**, *68*, 932–941. [CrossRef]
51. Revil, A.; Glover, P.W.J. Theory of ionic-surface electrical conduction in porous media. *Phys. Rev.* **1997**, *B55*, 1755–1773. [CrossRef]
52. Ge, S.; Gorelick, S.M. Groundwater and surface water. In *Encyclopedia of Atmospheric Sciences*, 2nd ed.; North, G.R., Pyle, J., Zhang, F., Eds.; Elsevier: Amsterdam, The Netherlands, 2015; Volume 3, pp. 209–216. [CrossRef]
53. Guerra, M. Aquitard. In *Encyclopedia of Engineering Geology*; Bobrowsky, P.T., Marker, B., Eds.; Encyclopedia of Earth Sciences Series; Springer: Charm, Switzerland, 2018. [CrossRef]
54. Oyeyemi, K.D.; Aizebeokhai, A.P.; Metwaly, M.; Oladunjoye, M.A.; Bayo-Solarin, B.A.; Sanuade, O.A.; Thompson, C.E.; Ajayi, F.S.; Ekhaguere, O.A. Evaluating the groundwater potential of coastal aquifer using geoelectrical resistivity survey and porosity estimation: A case in Ota, SW Nigeria. *Groundw. Sustain. Dev.* **2021**, *12*, 100488. [CrossRef]
55. Cheremisinoff, N.P. Pronciple of Hydrogeology. In *Groundwater Remediation and Treatment Technologies*, 1st ed.; Elsevier: Amsterdam, The Netherlands, 1998; pp. 85–126, eBook; ISBN 9780815517337.
56. Oteri, A.U.; Atolagbe, F.P. Saltwater Intrusion into Coastal Aquifers in Nigeria. In Proceedings of the Second International Conference on saltwater intrusion and coastal Monitoring, Modelling, and Management, Merida, Yucatan, Mexico, 31 March–2 April 2003.
57. Olufemi, A.G.; Utieyin, O.O.; Adebayo, O.M. Assessment of groundwater quality and saline intrusions in coastal aquifers of Lagos metropolis, Nigeria. *J. Water Resour. Prot.* **2010**, *2*, 849–853. [CrossRef]
58. Ojuri, O.; Bankole, O. Groundwater vulnerability assessment and validation for a fast growing city in Africa: A case study of Lagos, Nigeria. *J. Environ. Prot.* **2013**, *4*, 454–465. [CrossRef]
59. Ayolabi, E.A.; Folorunso, A.F.; Odukoya, M.A.; Adeniran, A.E. Mapping the saline water intrusion into the coastal aquifer with geophysical and geochemical techniques: The University of Lagos campus case (Nigeria). *Springerplus* **2013**, *2*, 433. [CrossRef] [PubMed]
60. Oyeyemi, K.D.; Aizebeokhai, A.P.; Oladunjoye, M.A. Integrated and geochemical investigations of saline water intrusion in a coastal alluvial terrain, Southwestern Nigeria. *Int. J. Appl. Environ. Sci.* **2015**, *10*, 1275–1288.
61. Kumar, H.; Tajdarul, H.S.; Amelung, F.; Agrawal, F.; Venkatesh, A.S. Space-time evolution of the National Capital Region of India using ALOS-1 and Sentinel-1 SAR data: Evidence of overexploitation. *J. Hydrol.* **2022**, *605*, 27329. [CrossRef]
62. Suganthi, S.; Elango, L. Estimation of groundwater abstraction induced land subsidence by SBAS technique. *J. Earth Syst. Sci.* **2020**, *129*, 46. [CrossRef]
63. Saber, M.; Abdel-Fattah, M.; Kantoush, S.A.; Sumi, T. Implications of land subsidence due to groundwater over-pumping: Monitoring methodology using Grace data. *Int. J. GEOMATE* **2018**, *14*, 52–59. [CrossRef]
64. Guzy, A.; Malinowska, A.A. State of the Art and Recent advancements in the modelling of land subsidience induced by groundwater withdrawal. *Water* **2020**, *12*, 2051. [CrossRef]
65. Taftazani, R.; Kazama, S.; Takizawa, S. Spatial Analysis of Groundwater Abstraction and Land Subsidence for Planning the Piped Water Supply in Jakarta, Indonesia. *Water* **2022**, *14*, 3197. [CrossRef]
66. Li, H.; Zhu, L.; Guo, G.; Zhang, Y.; Dai, Z.; Li, X.; Chang, L.; Teatini, P. Land subsidence due to groundwater pumping: Hazard probability assessment through the combination of Bayesian model and fuzzy set theory. *Nat. Hazards Earth Syst. Sci.* **2021**, *21*, 823–835. [CrossRef]

67. Ezquerro, P.; Guardiola-Albert, C.; Herrera, G.; Fernández-Merodo, J.A.; Béjar-Pizarro, M.; Bonì, R. Groundwater and Subsidence Modeling Combining. Geological and Multi-Satellite SAR Data over the Alto Guadalentín Aquifer (SE Spain). *Geofluids* **2017**, *2017*, 1359325. [CrossRef]
68. Guzy, A. Groundwater Withdrawal-Induced Land Subsidence. *Encyclopedia* **2020**. [CrossRef]
69. Garg, S.; Motagh, M.; Indu, J.; Karanam, V. Tracking hidden crisis in India's capital from space: Implications of unsustainable groundwater use. *Sci. Rep.* **2022**, *12*, 651. [CrossRef] [PubMed]